Genetic Diversity of Principal Neurons in the Hippocampus

Inauguraldissertation

Zur
Erlangung der Würde eines Doktors der Philosophie
vorgelegt der
Philosophisch-Naturwissenschaftlichen Fakultät
der Universität Basel

von

Yuichi Deguchi
aus Japan

Basel, 2009

Genehmigt von der Philosophisch-Naturwissenschaftlichen Fakultät

auf Antrag von

Prof. Dr. Pico Caroni
(Dissertationsleitung)

Prof. Dr. Silvia Arber
(Korreferat)

Dr. Botond Roska
(Experte)

Basel, den 10. 11. 2009

Prof. Dr. Eberhard Parlow
(Dekan)

Table of contents

Abbreviations ---------- 4

1. Introduction

1.1 Overview ---------- 5

1.2 Hippocampus anatomy ---------- 6

1.3 Hippocampus functions ---------- 7

1.4 Hippocampus along the dorsoventral axis ---------- 9

1.5 Gene expression patterns in the hippocampus ---------- 10

1.6 Genetic tools to dissect the neuronal circuit ---------- 11

2. Results

2.1 Selective connectivity among matched hippocampal principal neuron subpopulations ---------- 14

2.2 additional data

Overview ---------- 48

2.2.1 Distribution patterns of GFP-positive cells ---------- 48

2.2.2 The chromosomal location of the transgene in Lsi3 mice ---------- 50

2.2.3 HDAC inhibitor treatments in hippocampal slice cultures ---------- 51

2.2.4 Sexual dimorphisms in the hippocampus ---------- 56

3. Discussion and Conclusion

3.1 The subpopulations in the hippocampus ---------- 62

3.2 Genetic backbones of subpopulations ---------- 63

3.3 Genetic approach to dissect the neuronal circuits ---------- 64

3.4 Sexual dimorphisms in the hippocampus ---------- 65

3.5 Conclusions and further consideration ---------- 67

4. Supplementary materials and methods

4.1 Microarray analysis ---------- 69

4.2 In situ hybridization ---------- 69

4.3 3D reconstruction of the adult hippocampus ---------- 70

4.4 FISH (fluorescence in situ hybridization) ---------- 70

4.5 Hippocampal slice culture ---------- 71

5. References ---------- 72

Acknowledgements ---------- 78

Curriculum Vitae ---------- 79

Abbreviations

BCIP 5-bromo-4-chloro-3-inodolyl-phosphate
CA corpus ammonis (hippocampal region)
DG dentate gyrus (hippocampal region)
DIG digoxigenin
DIV day in vitro
GFP green fluorescent protein
EC entorhinal cortex
FISH fluorescent *in situ* hybridization
HDAC histone deacetylase
HOX homeobox
MAP2 microtubule-associated protein 2
NMDA N-methyl-D-aspartate
Rps9 ribosomal protein S9
OR olfactory receptor
Stx3 syntaxin 3
Thy1 thymus cell antigen 1, theta
TSA trichostatin A
UTR untranslated region

1. INTRODUCTION

1.1 Overview

In order to understand how neural circuits process information, it is important to identify the genetic subpopulations that make up the circuits and elucidate their individual connectivities and functions. For example, in the olfactory system, individual olfactory sensory neurons express only one odorant receptor (OR) gene, and sensory neurons expressing the same odorant receptor converge upon the same glomeruli (Buck and Axel, 1991; Ngai et al., 1993; Ressler et al., 1994). These findings have significantly contributed to understand how the olfactory system processes the information from different odors. Another well-dissected system is the mouse retina, where parallel ON and OFF pathways consist of distinct layers of interconnected neurons that exhibit distinct responses to light stimuli (Wässle, 2004). In the adult retina, subpopulations of ON or OFF bipolar cells connect selectively to subpopulations of ON or OFF ganglion cells (Wässle, 2004). Although activity plays a role in establishing these selective connections, current evidence that the genetically based cell identity of each subpopulation has a major role in establishing synaptic specificity in this circuit during development (Kerschensteiner et al., 2009).

The specification of motor neuron subpopulations and their selective connectivities to particular muscles was also studied extensively at the molecular level. There are several steps to specify these subpopulations, including the combinatorial expression of homeobox (HOX) genes, that of LIM-homeodomain transcription factors (TFs), the expression of intermediate TFs based on HOX genes, and the expression of TFs induced by peripheral signals (Jessell, 2000; Sanguinetto, 2008) (Fig.1). Interestingly, early-born neurons influenced the specification of late-born neurons in this system (Jessell, 2000) (Fig.1).

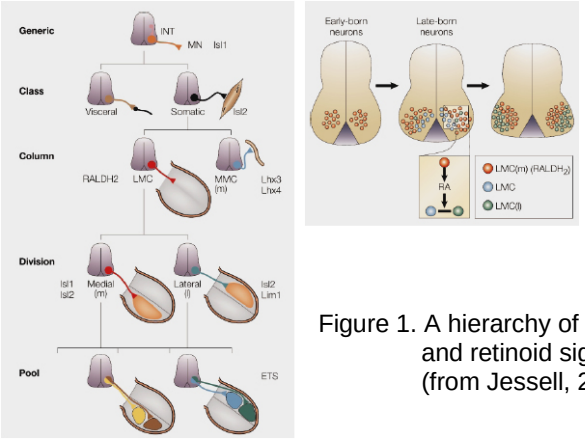

Figure 1. A hierarchy of motor neuron identities and retinoid signaling by early-born neurons (from Jessell, 2000)

Comparable studies as to whether there may be principal neuron subpopulations in the hippocampus, and whether this may affect their connectivities have not been available, and their investigation forms the object of this thesis work.

1.2 Hippocampus anatomy

Structurally, the hippocampus can be divided into three main subregions: dentate gyrus (DG), CA3 and CA1. The principal neuron in the DG is called the granule cell, which receives its main input from the entorhinal cortex (EC), and projects to CA3. In the hippocampus of a rat, there are around 1.2 million of granule cells (West et al., 1991). In the CA3 region, the principal neuron is called the CA3 pyramidal cell, which receives its main inputs from granule cells and from the EC, and projects to CA1. In the CA1 region, the principal neuron is called CA1 pyramidal cell, which gets its main inputs from CA3 pyramidal cells and from the EC, and sends output to the EC via the subiculum or directly. In all three regions, principal neurons form distinct layers, which are densely-packed. (Fig.1)

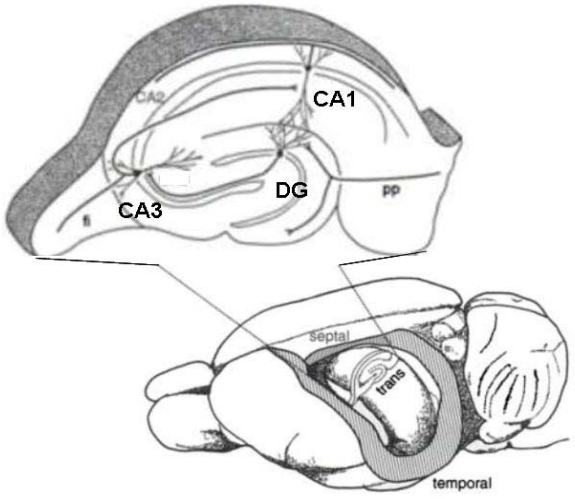

Figure 1. anatomy of hippocampus (modified from Andersen P. et al. 2007)

1.3 Hippocampus functions

There are many lines of evidence suggesting that the hippocampus plays an important role in learning and memory in mammals, including the mouse and man. One famous example is the case of HM. In this case, most of the hippocampus of the patient had to be removed because of epilepsy. After the surgery, early memories were normal and there was no impairment of personality or general intelligence. However, new long-term memory was not acquired (Scoville and Milner, 1957). Therefore, it was suggested that the hippocampus plays an important role in acquiring new episodic memories, but not in storing long-term memories like neocortex.

People's performance on many learning and memory tasks improves following sleep, especially slow-wave sleep (Marshall et al., 2006). It has been hypothesized that this improvement is due to interactions between the hippocampus and neocortex during sleep, leading to a transfer of newly acquired representations from the hippocampus to neocortex to form long-term memories.

Recent studies have provided evidence that the hippocampus plays an important role especially in spatial representation and spatial memory in several mammalian species (Moser et al., 2008). In the hippocampus, it was demonstrated that there were "place cells", which exhibited a high rate of firing whenever an animal was in a certain place, the so-called "place field" (O'Keefe and Dostrovsky, 1971). It was also suggested that the hippocampus encoded not only spatial information, but also temporal information about events (Hampson et al., 1993). In fact, the sequences of firing patterns of multiple CA1 pyramidal cells during the awake experience were replayed in the same sequences of firing patterns during sleep (Lee and Wilson, 2002).

Using mouse genetics it could be shown that each subregion of the hippocampus has its particular functions. For example, NMDA receptors in DG are important for pattern separation (McHugh et al., 2007). NMDA receptors of CA3 or CA1 pyramidal cells are necessary for associative memory recall and memory formation respectively (Nakazawa et al., 2002; Tsien et al., 1996). In these experiments, the critical step was to produce transgenic mice which express Cre recombinase only in the specific subregion of the hippocampus (Fig2).

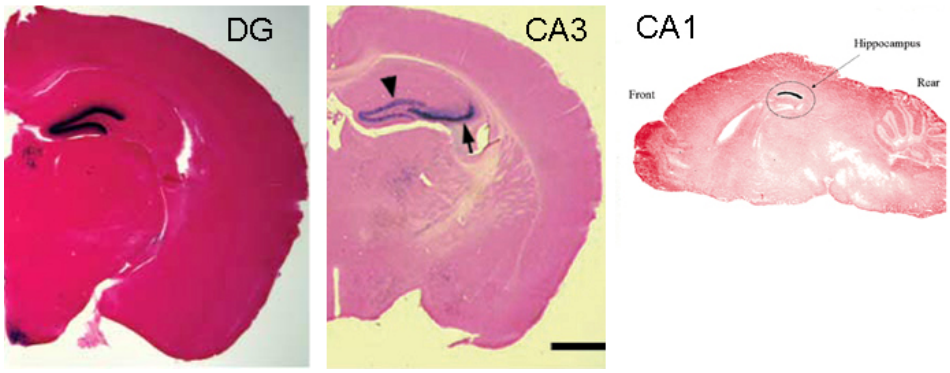

Figure 2. Specific Cre expression patterns in the each transgenic line.
(from Nakazawa et al., 2002; Tsien et al., 1996; McHugh et al., 2007)

1.4 Hippocampus along the dorsoventral axis

Early anatomical studies have provided evidence that the afferent and efferent connectivities of the hippocampus change along its dorsoventral axis. In rodents, the dorsal half of the hippocampus receives inputs from the lateral and caudomedial portion of the entorhinal cortex, and tends to send outputs to the lateral entorhinal cortex and dorsal lateral septum (Sahay and Hen, 2007) (Fig.3). On the other hand, the ventral half of the hippocampus receives mainly inputs from the rostromedial entorhinal cortex, and sends projections to the prefrontal cortex, the amygdala and nucleus accumbens, as well as the medial entorhinal cortex (Sahay and Hen, 2007) (Fig.3). The hippocampus also has distinct connectivities with other brain regions between dorsal and ventral regions of the hippocampus.

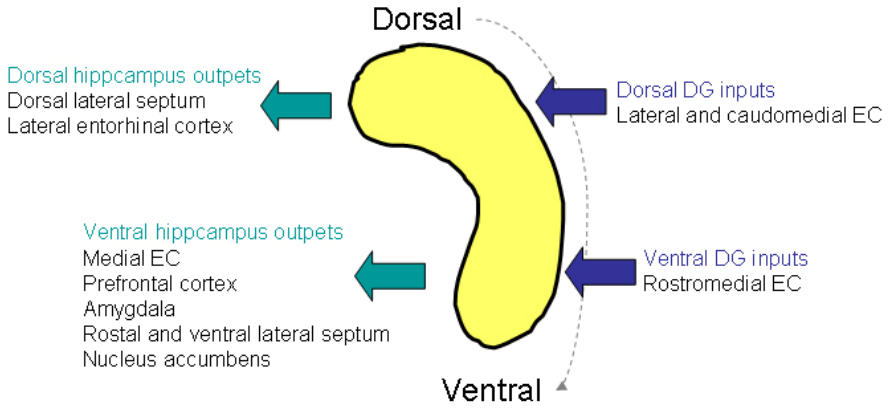

Figure 3. differential connectivity of the hippocampus along the dorsoventral axis

CA3 pyramidal cells also have well-defined place fields, and the scale of representation increases almost linearly from the dorsal region to the ventral region (Kjelstrup et al., 2008). Partial hippocampal lesion experiments have provided evidence that the dorsal hippocampus is critically important for spatial learning, whereas the ventral hippocampus is not (Moser and Moser, 1998; Sahay and Hen, 2007).

These evidences suggest that the hippocampus has discrete functions in its dorsal and ventral subdivisions. This gives rise to the possibility that the principal neurons in the hippocampus are not homogenous along the dorsoventral axis.

1.5 Gene expression patterns in the hippocampus

Recent studies have showed that there is specific regional or cellular regulation of gene expression patterns in the hippocampus. Some genes were exclusively expressed in a particular subregion of the hippocampus, e.g. in DG, CA3 or CA1 (Lein et al., 2004). Furthermore, the Allen Institute for Brain Science provided *in situ* hybridization data for more than 20,000 genes throughout the whole brain, including the hippocampus (Lein et al., 2007). These data allowed to identify molecular domains in the hippocampus characterized by the expression of specific combinations of genes (Thompson et al., 2008) (Fig.4). Interestingly, these molecular domains corresponded to extra- and intrahippocampal connectivity patterns (Thompson et al., 2008) (Fig.4).

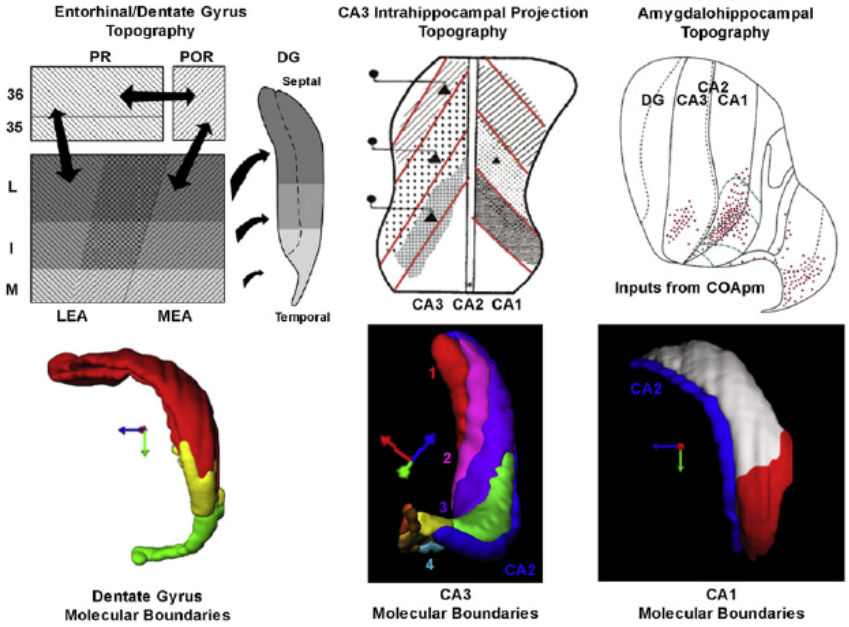

Figure 4. Concordance between molecular domains and hippocampal connectivity (from Thompson et al., 2008)

It was also demonstrated through single-cell microarray analysis that individual CA1 pyramidal cells can exhibit cellular heterogeneity at the gene expression level (Kamme et al., 2003).

These findings indicate that principal neurons in the hippocampus are not homogeneous at the molecular level. However, these studies did not clarify whether or not there may be distinct subpopulations of principal neurons in the hippocampus.

1.6 Genetic tools to dissect the neuronal circuit

Since neurons and their processes are densely packed in the nervous system, little information about individual neurons can be obtained if all of them are labeled. This has led to efforts to analyze smaller subsets of neuronal populations. The first successful method was discovered by Camillo Golgi in the 19th century. The Golgi staining can label a small population of neurons and almost completely visualize their dendritic and axonal processes. Although the Golgi staining had enormous impact for neuroscience, there were also limitations. For example, it does not label reliably all axonal branches and fine terminal arborizations, and it cannot be used for live tissue experiments. To overcome these limitations, several transgenic mice which expressed the fluorescent proteins or *lacZ* were generated (Caroni, 1997; Feng et al., 2000; Martin et al., 2002; Zong et al., 2005; Livet et al., 2007). One strategy is to label particular neuronal lineages (Martin et al., 2002; Zong et al., 2005). Using site-specific interchromosomal recombination, Mosaic Analysis with Double Markers (MADM), it was demonstrated that the lineage of neurons plays a role in directing the axonal projection pattern of granule cells in the mouse cerebellum (Zong et al., 2005). A clonal analysis was also done in the hippocampus, where experimental mouse chimeras expressing *lacZ* demonstrated that there may be specific distribution patterns of neurons belonging to the same lineage (Martin et al., 2002) (Fig.5).

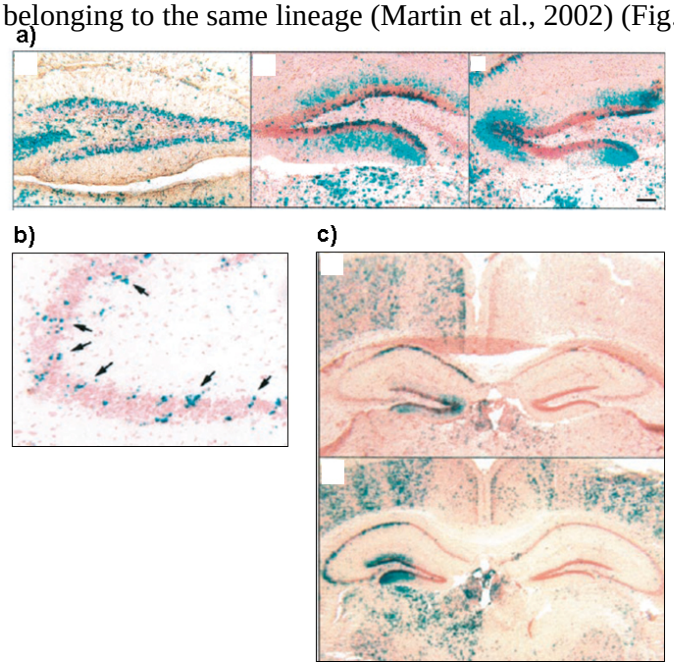

Figure 5. The distribution patterns of lacZ positive cells (modified form Martin et al., 2002) a) dentate gyrus, b) CA3 pyramidal cells, c) the hippocampus and other brain structures

A different strategy to label small populations of neurons is to generate transgenic mice expressing fluorescent proteins under the Thy1 promoter (Caroni, 1997; Feng et al., 2000; Livet et al., 2007). Although only small fractions of neurons in the hippocampus are labeled in these transgenic mice, it had remained unclear whether neurons are labeled in a random manner, or whether the patterns may reflect the existence of specific subpopulations in the hippocampus. This thesis tried to address this question, and at the same time to address the larger question of whether principal neurons in the hippocampus may be subdivided into genetically defined subpopulations. In order to address this question, three transgenic mice: Lsi1, Lsi2 and Lmu1 expressing membrane GFP under the Thy1 promoter were analyzed (Caroni, 1997). In Lsi1 or Lsi2 mice, some (5-25 % of total) granule cells, CA3 and CA1 pyramidal cells are GFP-positive in the hippocampus (Fig.6). On the other hand, all granule cells and CA1 pyramidal cells are GFP-positive and around 50 % CA3 pyramidal cells are GFP-positive in the Lmu1 line (Fig.6).

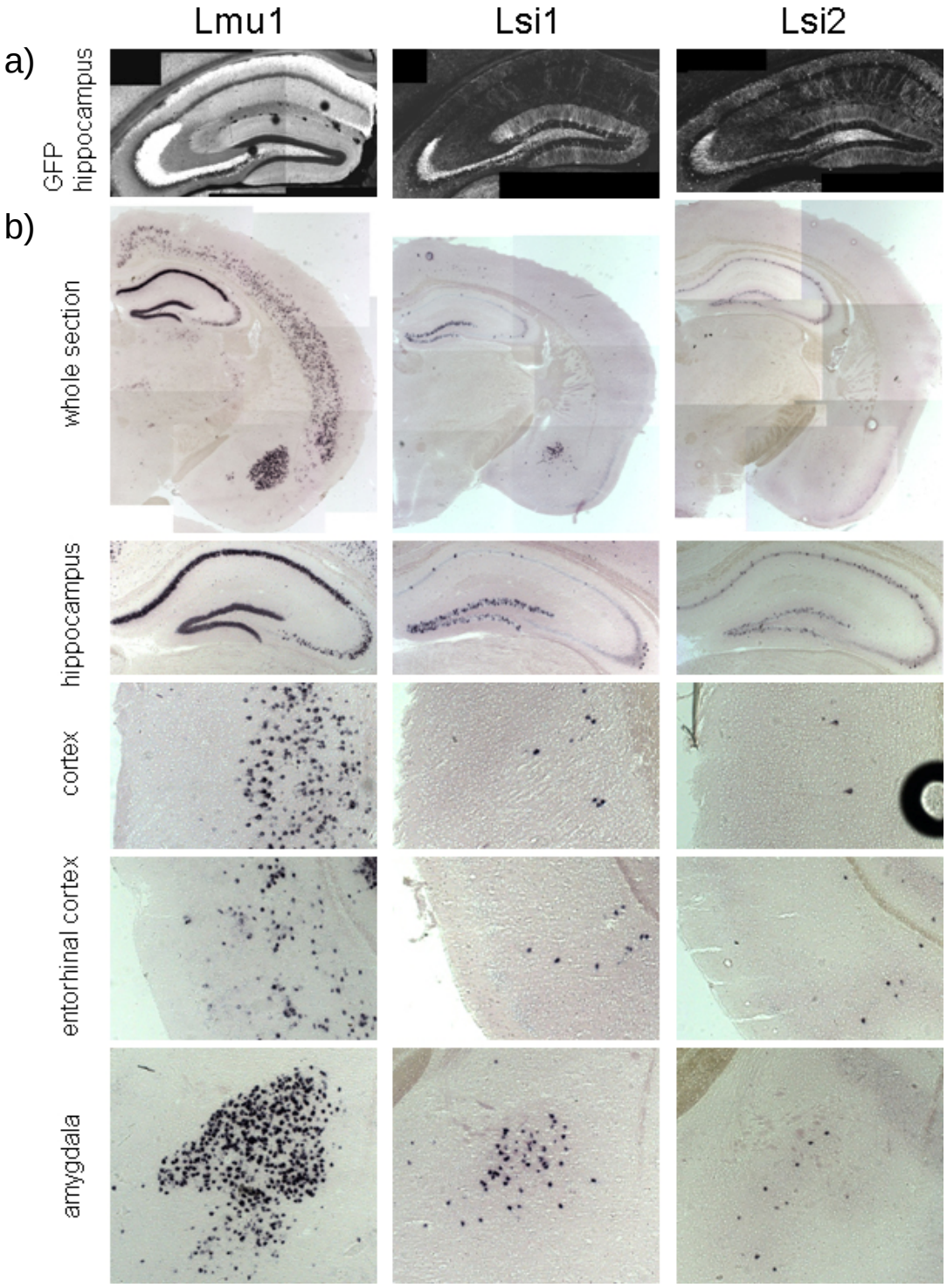

Figure 6 the distribution patterns of GFP-positive cells in Lmu1, Lsi1 or Lsi2 mice
a) GFP signal in the hippocampus b) *in situ* hybridization for GFP

2. Results 2.1 submitted

SELECTIVE CONNECTIVITY AMONG MATCHED HIPPOCAMPAL PRINCIPAL NEURON SUBPOPULATIONS

Yuichi Deguchi[1], Flavio Donato[1], Ivan Galimberti[1], Erik Cabuy, and Pico Caroni

Friedrich Miescher Institute, Maulbeerstrasse 66, CH-4058 Basel, Switzerland

[1]These authors contributed equally to the work

Send correspondence to:

Pico Caroni

Friedrich Miescher Institute, Maulbeerstrasse 66, CH-4058 Basel, Switzerland

email: caroni@fmi.ch tel: 0041 61 6973727 Fax: 0041 61 6973976

The extent to which individual neurons are interconnected in a selective manner within brain circuits is an unsolved problem in neuroscience. Two opposite views posit dedicated labeled lines of specifically interconnected neurons, versus tabula rasa models of randomly interconnected networks. Even in dense mammalian cortical circuits, apparently equivalent neurons can be organized into preferentially interconnected microcircuits. However, it has remained unclear whether microcircuits might reflect genetically defined subpopulations of selectively interconnected neurons, as opposed to self-organizing random networks. Here we show that the principal neurons of the major hippocampal subdivisions consist of genetically distinct subpopulations that interconnect selectively across subdivisions. In two Thy1 mouse lines, transgene expression in each subdivision visualizes matched principal neuron subpopulations that exhibit unique patterns of gene expression, and share neurogenesis windows, and temporal schedules of synaptogenesis. Marker genes shared among the matched subpopulations map near olfactory receptor gene clusters, a property which we find preferentially associated with neuronal subtype markers. Matched subpopulations exhibit selective connectivity at mossy fiber-to-pyramidal neuron synapses in CA3. Our results provide genetic, developmental and anatomical evidence for the existence of selectively interconnected principal neuron subpopulations in a cortical structure. The results further suggest that unique and co-ordinate schedules of neurogenesis and circuit assembly may underlie the establishment of specific microcircuits in the brain.

There is now compelling evidence for selective connectivity in cortical circuits[1-8], but whether this selectivity may involve specific subpopulations of neurons has remained unclear[1,9]. Investigating microcircuits has posed unique technical challenges due to the vast numbers of neurons and synapses in central neuropil[1,3,7]. Transgenic mouse lines based on a modified mouse Thy1.2 promoter cassette have produced stable expression patterns restricted to subgroups of neurons in the adult[10]. In „sparse“ Thy1 lines, high-level transgene expression in few neurons within several neuronal populations has been widely exploited to trace and image neuronal processes and their synaptic connections at high resolution[11,12]. Notably, although the lines exhibit clear variegations effects (i.e. unpredictable variations in the numbers of transgene-expressing neurons among individuals of the same mouse line), the distribution of labeled cells in these Thy1 lines is not entirely random. For example, in three different „sparse“ lines, transgene expression among retinal amacrine cells was restricted to very few defined subtypes[13]. „Sparse“ Thy1 lines may thus provide suitable tools to investigate whether defined subpopulations of neurons establish selective synaptic connections.

The principal tri-neuronal circuit in the hippocampus, which relays granule cells (GCs) in the dentate gyrus (DG) to pyramidal neurons in CA3 and then pyramidal neurons in CA1, provides an attractive system to investigate the notion of subpopulations of selectively interconnected neurons in cortical structures. Thus, there is a wealth of anatomical and functional information about hippocampal circuits[14-17]. Furthermore, principal neurons in the hippocampus are well segregated into layers, and exhibit prominent transgene expression in „sparse“ Thy1 lines[12,14]. We therefore used the two „sparse“ Thy1 reporter lines Lsi1 and Lsi2, which overexpress membrane-targeted GFP (mGFP) in few neurons[12,18], to investigate the possible existence and the connectivities of principal neuron subpopulations in the hippocampus.

Molecularly distinct principal neuron subpopulations

To investigate the possibility that mGFP-positive neurons in Lsi1 and Lsi2 mice may visualize subpopulations of principal neurons in the hippocampus, we

analyzed their transcriptomes in the adult, their appearance during hippocampal neurogenesis, and their maturation during the establishment of hippocampal circuits. These three properties of Lsi1 and Lsi2 neurons were compared to those of a random population of principal neurons in DG, CA3 and CA1. In the second part of the study we analyze the connectivities between mGFP-positive GCs and CA3 pyramidal neurons in Lsi1 and Lsi2 mice (**Supplementary Fig. 1**).

We first analyzed gene expression patterns of transgene-positive hippocampal GCs in adult Lsi1 and Lsi2 mice. Forty-to-fifty mGFP-positive cells were collected individually from three defined hippocampal positions using laser-dissection microscopy, and then analyzed as pools on Affimetrix chips[19]. The procedure was repeated for a total of 3 Lsi1 and Lsi2 mice each, at 2, 4, 8 and 16 weeks of age. For comparison, similar sets of GCs were collected from 3 Lmu1 Thy1 mice, which exhibit broad expression of mGFP in the DG[12] (**Supplementary Fig. 2**). When compared to average values, Lsi1 and Lsi2 GCs each exhibited 150-250 genes which were either up- or downregulated at least 2-fold at 16 weeks ($p<0.05$; **Fig. 1a**; **Supplementary Fig. 3**). Some of the genes downregulated in Lsi1 or Lsi2 GCs exhibited expression values >50-fold lower than the average population, and some genes were altered in opposite ways in Lsi1 and Lsi2 GCs (**Supplementary Fig. 4**). The range within which the fractions of transgene-expressing GCs over total numbers of GCs varied in individual transgenic mice was 3-20% (Lsi1), and 1-15% (Lsi2) (N=50 mice each), but gene enrichment values over average GCs were closely comparable in GCs from mice with different frequencies of transgene-positive neurons (**Fig. 1b**), suggesting that the fractions of Lsi1 and Lsi2 GCs in DG may be at least 20%, respectively 15%.

Transgene-positive hippocampal CA3 and CA1 pyramidal neurons in Lsi1 and Lsi2 mice also exhibited unique gene expression patterns (**Fig. 1c**; **Supplementary Fig. 5**). Like for GCs, the subpopulation patterns of gene expression were independent from the frequencies of transgene-expressing cells in individual mice (**Fig. 1c**). To carry out a non-biased subpopulation test based on gene expression profiles, we took a group of 492 genes, consisting of 100 genes with the highest deviations from average values at 16 weeks in either Lsi1 or Lsi2 GCs, CA3 pyramidal neurons or CA1 pyramidal neurons (total of 600 genes, minus 108 overlaps), and used the genes to

analyze the combined gene profiling databases including four different postnatal ages (2w, 4w, 8w, 16w), thus generating hierachical trees of cell type relatedness (i.e. determining which cell type/genotype/age samples are most related to another). With the exception of the 2 weeks samples, where developmental aspects were apparently predominant, this unbiased in silico test for relatedness consistently separated Lsi1 and Lsi2 principal neurons from average populations, irrespective of age (**Fig. 1d**).

Matched subpopulations in DG, CA3 and CA1

Among the transcripts specifically regulated in opposite ways in Lsi1 and Lsi2 principal neurons, a small group was shared among GCs in the DG, and pyramidal neurons in CA3 and CA1 (**Fig. 2a**). These included a 3' UTR splicing variant of Syntaxin 3 (STX3(3'); excluded from Lsi2 neurons, enriched in Lsi1 neurons), and a 3' UTR sequence of ribosomal protein S9 (S9(3'); excluded from Lsi1 neurons, enriched in Lsi2 neurons) (**Fig. 2a**). Double-in situ hybridization of hippocampal sections confirmed these relationships at the level of individual neurons, thus providing evidence that Lsi1 and Lsi2 subpopulations are homogeneous with respect to the expression of subsets of genes (**Fig. 2b**). For clarity, we will designate the entire Subpopulation of potentially Lsi1- or Lsi2-positive Hippocampal Principal neurons as HP(Su1), respectively HP(Su2) neurons. HP(Su1) neurons are thus (STX3(3')+, S9(3')-), whereas HP(Su2) neurons are (STX3(3')-, S9(3')+).

To investigate what might underlie the visualization of hippocampal principal neuron subpopulations in „sparse" Thy1-mGFP transgenic mice, we determined the insertion sites of the transgenes in these mice. In Lsi1 mice, Thy1-mGFP transgene copies had inserted at one single locus, near the centromere on chromosome 16 (**Supplementary Fig. 6**). Lsi2 mice also exhibited transgene copies near the centromere, but on chromosome 19 (**Supplementary Fig. 6**). Centromeric regions exhibit compacted chromatin consistent with pronounced transgene silencing. In addition, the two particular chromosomal insertion sites correspond to two of the only four centromeric regions in the mouse genome that exhibit an Olfactory Receptor (OR) gene cluster in their vicinity[20] (less than 15 MB from centromeric edge; **Supplementary Fig. 6**). By contrast, the single transgene insertion site in Lmu1 mice was located on chromosome 2, neither near a centromere, nor near an OR cluster

(**Supplementary Fig. 6**). A survey of published neuronal types and subtypes marker genes revealed that the latter have a high probability to map near OR sites. Thus, from a list of genes specifically expressed in major cortical or retinal cell types, all of them were more than 10 MB away from an OR cluster, whereas 48.5% (respectively 74%) of a subtype marker[21,22] list mapped within 1 MB (respectively 5 MB) from an OR cluster (**Fig. 2c**; **Supplementary Fig. 7**). We then determined the extent to which shared HP(Su1)- and HP(Su2)-selective genes are located near OR clusters. When 400 genes were picked randomly among those expressed in all GCs, 4.8% of the genes mapped within 1 MB from an OR cluster (**Fig. 2c**). Genes varying within Lsi1 GCs between 8 weeks and 16 weeks exhibited similar low correlations to OR clusters (3.8% within 1 MB; F**ig. 2c**). By contrast, when only genes up- or down-regulated in all HP(Su1) or HP(Su2) neurons (i.e. in DG, CA3 and CA1) were considered, 52% of them mapped within 1 MB of an OR cluster (**Fig. 2c**). These shared genes were regulated in a closely comparable manner in transgene-positive neurons in DG, CA3, CA1 (**Fig. 2d**). Furthermore, OR vicinities were maximised, when only genes up-regulated 4-5-fold or down-regulated more than 5-fold in Lsi1 or Lsi2 neurons were included in the analysis (e.g. for >2x versus >5x down in Lsi1: 6.8% versus 23% within 1 MB; **Fig. 2c**). Therefore, like neuronal subtype marker genes, genes specifically enriched in HP(Su1) or HP(Su2) principal neurons have a high probability to map near OR clusters.

Matched spatio-temporal patterns of neurogenesis

We next analyzed the temporal patterns of HP(Su1) and HP(Su2) neurogenesis in Lsi1 and Lsi2 mice. We injected mice with BrdU at defined times during embryonic development or early postnatally, and analyzed hippocampal sections from 1 month-old mice for BrdU labeling and mGFP signals[23]. Only strongly BrdU labeled cells that did not undergo further rounds of DNA replication and cell division subsequent to BrdU incorporation were included in the analysis. Consistent with previous reports, the overall population of GCs was generated during two broad rounds of neurogenesis, one peaking between E12 and E15, and the second one peaking between P3 and P7[24-26] (**Fig. 3a**). Lsi1 GCs exhibited sharper temporal neurogenesis patterns, with peaks within the earlier 25% of each granule cell neurogenesis wave (**Fig. 3a**). Lsi2 GCs were produced with a shift of about 2 days

compared to their Lsi1 counterparts, but still within the first half of the embryonic and postnatal neurogenesis waves (**Fig. 3a**). No Lsi1 or Lsi2 GCs were detected among adult born GCs (0/240 Doublecortin-positive GCs in 3 mice each, at 4 months). In close correspondence to Lsi1 GCs, Lsi1 CA3 and CA1 pyramidal neurons were produced during the earliest phase of their corresponding neurogenesis processes (**Fig. 3b**). Lsi2 CA3 pyramidal neurons were produced during a defined early window of developmental time, slightly later than Lsi1 neurons, whereas for CA1 pyramidal neurons Lsi2 and Lsi1 overlapped extensively (**Fig. 3b**). When different individuals from the same mouse line were compared, varying total numbers of Lsi1 or Lsi2 mGFP-positive GCs (or pyramidal neurons) did not affect the fractions of transgene-positive cells produced during any neurogenesis interval (**Figs. 3a, b**), suggesting that variegation effects only influenced the probability of mGFP expression within defined subpopulations of GCs.

We then investigated the specification of HP(Su1) and HP(Su2) subpopulations. In Lsi1 mice, pairs of mGFP-positive radial glia were already detected in the hippocampal neuroepithelium (HN) at E10.5, at a time preceding precursor neurogenesis[26-28] (**Fig. 3c**). Increasing numbers of transgene-positive postmitotic neuroblasts were detected along the HN at various distances from the presumptive Hem from E11.5 on, indicating the presence of Lsi1 GCs, CA3 pyramidal neurons, and CA1 pyramidal neurons[27] already at this early age (**Supplementary Fig. 8**). Comparable radially oriented groups of mGFP-positive cells were detected in Lsi2 embryos with a delay of 1-1.5 days of development (**Supplementary Fig. 8**). Systematic spatial mapping of labeled cells in several embryos at the same developmental time or in adult mice, revealed that mGFP-positive cells were distributed according to specific, reproducible and distinct patterns in the two lines of transgenic mice (**Supplementary Fig. 8**). Time lapse imaging of hippocampal explant cultures from Lsi1 embryos provided evidence that mGFP-positive postmitotic neuroblasts migrated and developed into GCs (**Supplementary Fig. 9**).

To determine whether Lsi1 neurons are representative of the earliest subpopulation of principal neurons during hippocampal neurogenesis, we compared spatial patterns of mGFP-positive cells to those of EdU-incorporating cells (a BrdU

analogue that can be visualized under non-denaturing conditions[29]). Between E11.5 and E12.5, spatial patterns of precursor neurogenesis (Tbr2+)[30] and of mGFP-positive Lsi neurons were closely comparable (**Fig. 3d**). Zones of early neurogenesis at E11.5[27,28] (EdU+) correponded to reproducible discrete territories depleted of Nestin- and Ki67-positive neuronal precursors 2 days later, and enriched in mGFP+ neuroblasts, suggesting that early hippocampal neurogenesis proceeded according to non-random spatial patterns (**Fig. 3d**). Consistent with the notion that Lsi1 neurons are representative of the earliest principal neurons in the hippocampus, neurons labeled with BrdU between E11.5 and E12.5, co-distributed with transgene-positive Lsi1 neurons in adult CA3 (**Supplementary Fig. 8**).

Matched distinct temporal patterns of synaptogenesis

To investigate how HP(Su1) and HP(Su2) subpopulations insert into hippocampal circuits, we analyzed the dendrites and axons of mGFP-expressing neurons between P5 and P10, during the early phases of adult hippocampal synaptogenesis[31]. A comparison of Lsi1 and Lsi2 CA3 pyramidal neurons suggested that Lsi1 neurons anticipated Lsi2 neurons by 2-4 days (**Fig. 4a**). Within CA3b, where earliest born Lsi2 neurons accumulate first, Lsi1 and Lsi2 pyramidal neurons were each homogeneous with respect to maturation, and exhibited no overlap in maturation or spinogenesis between P5 and P10 (**Fig. 4a**). Closely comparable maturation and spinogenesis patterns were detected for distal CA1 pyramidal neurons (next to subiculum; **Fig. 4a**). Consistent with these marked temporal differences in hippocampal circuit assembly, Lsi1 GCs downregulated the developmental markers[32] Doublecortin and Sema3C before Lsi2 GCs, and both subpopulations matured before the average of all GCs (**Fig. 4b**). Lsi1 mossy fibers established large mossy fiber terminals in stratum lucidum between P5 and P7, where these frequently contacted Lsi1 pyramidal neurons from P7 on (**Fig. 4c**). By contrast, no mossy fiber terminals were detectable along Lsi2 mossy fibers at P7; at P10, the terminals were rare and small, but they often contacted Lsi2 pyramidal neurons (**Fig. 4c**). Presynaptic patterns of synaptogenesis were also qualitatively different between Lsi1 and Lsi2 mossy fibers, with the latter establishing smaller terminals and being more prone to collateral formation (**Figs. 4c**; **Supplementary Fig. 10**). In parallel to a delay in mossy fiber synaptogenesis, dendritic development in Lsi2 GCs lagged by 3-4 days behind that in

Lsi1 GCs at all positions along the blades[31] (**Fig. 4c**). Comparable distinct timings, rates and patterns of presynaptic maturation were detected between Lsi1 and Lsi2 mossy fibers in organotypic slice cultures (**Supplementary Fig. 10**).

To provide independent evidence for the presence of distinct subpopulations of hippocampal principal neurons exhibiting pronounced differences in synaptic maturation, we analyzed transgene-positive CA3 pyramidal neurons and mossy fibers in Lmu1 mice. At P7, the analysis revealed the expected presence of subpopulations of mossy fibers and CA3 pyramidal neurons maturing in patterns comparable to those of HP(Su1) and HP(Su2) neurons, and that of additional transgene-positive neurons maturing after these early subpopulations of principal neurons (**Fig. 4d**).

Selective connectivity within principal neuron subpopulations

To determine whether matched HP(Su1) (or HP(Su2)) principal neurons exhibit synaptic contacts selectively with another, we analyzed contacts between mGFP-positive Lsi1 (or Lsi2) mossy fiber terminals and CA3 pyramidal neurons in adult mice. Only events in which the distance between mossy fiber terminals (>3 μm diameter) and pyramidal neuron dendrites was smaller than 0.2 μm were considered as putative contact sites. For more than 70% of these putative synaptic contacts, we determined whether mGFP/Bassoon accumulation sites (presynaptic) were apposed to mGFP/Pi-GluR1 puncta (postsynaptic) (**Supplementary Fig. 11**), and validated the vast majority of those putative synapses (48/50) by this procedure[18]. Due to the very low connectivity between GCs and pyramidal neurons in dorsal hippocampus[14], the likelyhood of finding such synaptic contacts by chance is extremely low. Nevertheless, a systematic analysis of 100 x 100 x 55 μm volumes yielded frequent contact sites between mGFP-positive cells (**Fig. 5a**). A statistical analysis revealed that the likelyhood that these frequencies were chance events was 10^{-5} or less (**Fig. 5a**). Comparable selective contacts between mGFP-positive GCs and CA3 pyramidal neurons were detected for Lsi2 neurons (**Fig. 5a**).

To determine whether principal neuron subpopulations related through their neurogenesis time windows in the DG and in CA3 may exhibit synaptic connections

selectively with another, we compared the distributions of Lsi1 mossy fiber terminals (early presynaptic subpopulation) to that of clusters of CA3 pyramidal neurons labeled in an unbiased manner with BrdU either at the beginning (early postsynaptic population; HP(Su1)-like) or at the end (late postsynaptic population; no overlap with HP(Su1)) of CA3 neurogenesis. As expected, mGFP-positive Lsi1 CA3 pyramidal neurons co-distributed with some, but not all clusters of „early labeled" pyramidal neurons (not shown), and clusters of Lsi1 mossy fiber terminals co-distributed with „early-labeled" pyramidal neuron clusters irrespective of whether they contained transgene-positive cells (**Fig. 5b**). By contrast, no Lsi1 mossy fiber terminal clusters co-distributed with „late labeled" pyramidal neuron clusters, which consistently coincided with mGFP-labeled mossy fiber stretches with little or no large mossy fiber terminals (**Fig. 5b**). These results suggest that early-born HP(Su1) mossy fibers selectively establish synaptic connections with early-born, but not with late-born pyramidal neurons in CA3.

To further investigate the notion that selective connectivity between Lsi1 or Lsi2 principal neurons in DG and CA3 is based on selective recognition processes between subpopulations of cells, we analyzed the connectivity of Lsi1 and Lsi2 neurons in a *Reelin*$^{-/-}$ background, where the cell layer organisations in hippocampal DG and CA3 are majorly disrupted[33]. As expected, the positions of GCs and CA3 pyramidal neurons, and the trajectories of mGFP-positive mossy fibers were obviously abnormal in the absence of Reelin (**Supplementary Fig. 11**). Transgene-expressing Lsi1 neurons now populated the outer layer of neocortex, supporting the notion that Lsi1 neurons maintained their identities in the absence of Reelin[33] (**Supplementary Fig. 11**). Notably, the disruption of hippocampal layer organization did not affect the frequencies by which Lsi1, respectively Lsi2 mossy fibers and CA3 pyramidal neurons established synaptic connections with each other (**Supplementary Fig. 11**).

Conclusions and implications

We have shown that matched principal neuron subpopulations in DG, CA3 and CA1 defined by their distinct patterns of gene expression, distinct early neurogenesis windows, and distinct timings of synaptogenesis, exhibit selective

connectivity at mossy fiber-to-pyramidal neuron synapses in CA3 (**Supplementary Fig. 1**). A detailed analysis of total Lsi1 and Lsi2 principal neuron numbers in the hippocampus provides further insights into how these subpopulations may be specified during development. Published figures of total principal neuron numbers in rat hippocampus, normalized to CA3, yield values of 1 (CA3), 4.8 (GCs) and 1.5 (CA1)[14]. Remarkably, corresponding values of total transgene-positive neurons were 1 (CA3), 4.4 ± 0.2 (GCs), and 1.5 ± 0.1 (CA1) for Lsi1, and 1 (CA3), 4.6 ± 0.1 (GCs), and 1.4 ± 0.1 (CA1) for Lsi2 (N=5 mice each; absolute numbers within each mouse line varying by a factor of up to 2.7). Therefore, total fractions of HP(Su1) (or HP(Su2)) neurons in the three main hippocampal subdivisions are closely comparable. These findings suggest that the subpopulations are specified through a mechanism that allocates fixed proportions of neurons within the neurogenesis processes that lead to principal neurons in DG, CA3 and CA1. The allocation is made early in neural development, and may manifest for each particular subpopulation as a probability function of time during neurogenesis.

Our findings that HP(Su1) and HP(Su2) neurons reflect two early subpopulations of hippocampal principal neurons are consistent with previous reports that neurons generated early during neurogenesis also mature and insert into circuits at faster rates[34,35]. It is tempting to speculate that selective connectivity within HP(Su1) and HP(Su2) neurons might be causally related to their temporally co-ordinate maturation, but further studies will be required to directly test this possibility. That distinct temporal sequences of neurogenesis are coupled to specific patterns of synaptogenesis has been shown conclusively for Drosphila[34-37], but no corresponding evidence had been reported for vertebrates.

To what extent may hippocampal connectivity be influenced by subpopulation specificities? A preliminary analysis revealed frequent contacts between matched mGFP+ CA3 and CA1 pyramidal neurons in our mice, but an assessment of selective connectivity in this part of the hippocampal circuit is more difficult due to the high degree of connectivity between these neurons[14]. However, if, as our findings suggest, temporally coincident maturation is a factor affecting synaptic specificity, outcomes may differ between sparse connectivity systems such as the mossy fiber to pyramidal neuron synapses in CA3, and highly interconnected systems like the recurrent

collaterals in CA3 or the Schaffer collaterals in CA1. Thus, for each subpopulation synaptogenesis in stratum lucidum was established rapidly, within 1-2 days, whereas synapse densities increased during at least 5 days in stratum radiatum and stratum lacunosum moleculare. Accordingly, specificities may be highest for low-density, fast assembling synapse systems. Timing-based schemes favoring selective synaptogenesis in rapidly maturing sparse systems may thus assign important roles to driver synapses[38] in circuit assembly and maturation. How the subpopulations and their microcircuits may have specific roles in hippocampal information processing remains to be determined.

Methods

Thy1 reporter mice were as described; reelin mutant mice were from Jackson's Laboratories. Antibodies: rabbit anti-GFP (Invitrogen), mouse anti-MASH1 (BD Pharmingen), mouse anti-Nestin and rabbit anti-Prox1 (Chemicon International), goat anti-NeuroD1 (Santa Cruz), rabbit anti-Tbr2/Eomes and rat anti-BrdU (Abcam).
The protocol for LDM collection and microarray analysis of few mGFP-labeled neurons was as described[19]. Average present call values were 40-48%. The double in situ hybridization protocol was as described[39]; signals from DIF or FITC labeled probes were amplified and detected using TSA plus Cyanine 3 or TSA plus Cyanine 5 system (PerkinElmer).
Immunocytochemistry was on PFA-fixed tissue (50 μm floating sections); detection was with Alexa 488, 568 and 647 conjugated antibodies (Molecular Probes). For analysis in the lamellar plane, hippocampi were dissected from perfused brains after O/N post-fixation, embedded in 3% agarose gel, and sliced transversally with a tissue chopper (McIlwain, 100 μm slices).
The BrdU labeling method in vivo was carried out in 24h intervals, as described[23]. EdU detection was as described[29] (Invitrogen Click-it EdU).
Maturity Scores were based on published immature/mature features[31], using 3D Imaris software. Individual features were assigned a value between 0 (least mature) and 3 (most mature), and values were summed. Parameters for dendrites were length,

diameter, diameter change at branchpoint, swellings, spines; axons: swellings, collaterals, filopodia, volume of terminals. For spine densities, only protrusions shorter than 2 μm, with an evident connection to the main shaft were included. Statistical differences were assessed by the student's t-Test.

To investigate transgene-positive mossy fiber / CA3 pyramidal neuron connectivities, lamellar sections were processed for immunocytochemsitry (Bassoon and Pi-GluR1), and non-overlapping CA3 stratum lucidum volumes containing mGFP+ pyramidal neurons were analyzed. Lengths were 100 μm (expect one terminal per 100-140 μm along CA3[14]) and depths were 55 μm. Average pyramidal neuron numbers within these volumes was 173 (dorsal third of hippocampus). For each mGFP+ pyramidal neuron within the volume we determined the number of putative synaptic contacts with mGFP+ mossy fibers. We then computed probability mass functions (binomial distributions) as follows: $Pr(K=k) = f(k; n; p) = (n!/k!(n-k)!)\ p^k(1-p)^{n-k}$, where k is number of connections found, n is (number of mGFP+ mossy fibers) x (average number of mGFP+ pyramidal neurons), and p is the probability for each contact (1/173; independent and identically distributed).

References

1. Brown, S.P. & Hestrin, S. Cell-type identity: a key to unlocking the function of neocortical circuits. *Curr. Op. Neurobiol.* **19**, 1-7 (2009)

2. Kozloski, J., Hamzei-Sichani, F. & Yuste R. Stereotyped position of local synaptic targets in neocortex. *Science* **293**, 868-72 (2001)

3. Yoshimura, Y. & Callaway, E.M. Fine-scale specificity of cortical networks depends on inhibitory cell type and connectivity. *Nat. Neurosci.* **8**, 1552-59 (2005)

4. Song, S., Sjostrom, P.J., Reigl, M., Nelson, S. & Chklovskii, D.B. Highly nonramdom features of synaptic connectivity in local cortical circuits. *PLoS Biol.* **3**e68 (2005)

5. Kampa, B.M., Letzkus, J.J. & Stuart, G.J. Cortical feed-forward networks for binding different streams of sensory information. *Nat.Neurosci.* **9**, 1472-3 (2006)

6. Brown, S.P. & Hestrin, S. Intracortical circuits of pyramidal neurons reflect their long-range axonal targets. *Nature* **457**, 1133-36 (2009)

7. Petreanu, L., Mao, T., Sternson, S.M. & Svoboda, K. The subcellular organization of neocortical excitatory connections. *Nature* **457**, 1142-45 (2009)

8. Yu, Y.C., Bultje, R.S., Wang, X. & Shi, S.H. Specific synapses develop preferentially among sister excitatory neurons in the neocortex. *Nature* **458**, 501-4 (2009)

9. Kalisman, N., Silberberg, G. & Markram, H. The neocortical microcircuit as a tabula rasa. *Proc. Natl. Acad. Sci. USA* **102**, 880-5 (2005)

10. Caroni, P. Overexpression of growth-associated proteins in the neurons of adult transgenic mice. *J. Neurosci. Meth.* **71**, 3-9 (1997)

11. Feng, G. *et al.* Imaging neuronal subsets in transgenic mice expressing multiple spectral variants of GFP. *Neuron* **28**, 41-51 (2000)

12. De Paola, V., Arber, S. & Caroni, P. AMPA receptors regulate dynamic equilibrium of presynaptic terminals in mature hippocampal networks. *Nat. Neurosci.* **6**, 491-500 (2003)

13. Haverkamp, S. *et al.* The primordial, blue-cone color system of the mouse retina. *J. Neurosci.* **25**, 5438-45 (2005)

14. Amaral, D. & Lavenex, P. Hippocampal neuroanatomy. in The Hippocampus Book (Andersen, P. *et al.* eds.) Oxford Univ. press pp. 37-110 (2007)

15. Lein, E. S., Zhao, X. & Gage, F.H. Defining a molecular atlas of the hippocampus using DNA microarrays and high-throughput *in situ* hybridization. *J. Neurosci.* **24**, 3879-89 (2004)

16. Thompson, C. L. *et al*. Genomic anatomy of the hippocampus. *Neuron* **60**, 1010-21 (2008)

17. Kamme, F. *et al.* Single-cell microarray analysis in hippocampus CA1: demonstration and validation of cellular heterogeneity. *J. Neurosci:* **23**, 3607-15 (2003)

18. Gogolla, N., Galimberti, I. Deguchi, Y., & Caroni, P. Wnt signaling mediates experience-related regulation of synapse numbers and mossy fiber connectivities in the adult hippocampus. *Neuron* **28**, 510-525 (2009)

19. Saxena, S., Cabuy, E. & Caroni, P. A role for motoneuron subtype-selective ER stress in disease manifestations of FALS mice. *Nat. Neurosci.* **12**, 627-36 (2009)

20. Godfrey, P. A., Malnic, B. & Buck, L. B. The mouse olfactory receptor gene family. *Proc. Natl Acad. Sci. USA* **101** 2156-61 (2004)

21. Dijk, F., Leeuwen, S. v. & Kamphuis, W. Differential effects of ischemia/ reperfusion on amacrine cell subtype-specific transcript levels in the rat retina. *Brain Res.* **1026**, 194-204 (2004)

22. Zylka, M. J., Rice, F. L. & Anderson, D. J. Topographically distinct epidermal nociceptive circuits revealed by axonal tracers targeted to *Mrgprd*. *Neuron* **45**, 17-25 (2005)

23. Wojtowicz, J.M. & Kee, N. BrdU assay for neurogenesis in rodents. *Nat. Protocols* **1**, 1399-405 (2006)

24. Li, G. *et al*. Hilar mossy cells share developmental influences with dentate granule neuron. *Dev Neurosci.* **30**, 255-61 (2008)

25. Altman, J. & Bayer, S.A. Migration and distribution of two populations of hippocampal granule cell precursors during the perinatal and postnatal periods. *J. Comp. Neurol.* **301**, 365-81 (1990)

26. Noctor, S.C., Flint, A.C., Weissman, T. A., Dammerman, R.S., & Kriegstein, A.R. Neurons derived from radial glia cells establish radial units in neocortex. *Nature* **409**, 714-20 (2001)

27. Altman, J. & Bayer, S.A. Mosaic organization of the hippocampal neuroepithelium and the multiple germinal sources of dentate granule cells. *J. Comp. Neurol.* **301**, 325-42 (1990)

28. Tole, S. & Grove, E.A. Detailed field pattern is intrinsic to the embryonic mouse hippocampus early in neurogenesis. *J. Neurosci.* **21**, 1580-9 (2001)

29. Chehrehasa, F., Meedeniya, A.C., Dwyer, P., Abrahamsen, G. & Mackay-Sim, A. EdU, a new thymidine analogue for labeling proliferating cells in the nervous system. *J. Neurosci. Meth.* **177**, 122-30 (2009)

30. Hodge. R.D. *et al.* Intermediate progenitors in adult hippocampal neurogenesis: Tbr2 expression and coordinate regulation of neuronal output. *J. Neurosci.* **28**, 3707-17 (2008)

31. Jones, S.P., Rahimi, O., O'Boyle, M.P., Diaz, D.L. & Claiborne, B.J. Maturation of granule cell dendrites after mossy fiber arrival in hippocampal field CA3. *Hippocampus* **13**, 413-27 (2003)

32. Tremblay, M.E., Riad, M., Chierzi, S., Murai, K.K., & Pasquale, E. Developmental course of EphA4 cellular and subcellular localization in the postnatal rat hippocampus. *J. Comp. Neurol.* **512**, 798-813 (2009)

33. Frotscher, M., Zhao, S. & Förster, E. Development of cell and fiber layers in the dentate gyrus. *Prog. Brain Res.* **163**, 133-42 (2007)

34. Petrovic, M. & Hummel, T. Temporal identity in axonal target layer recognition. *Nature* **456**, 800-3 (2008)

35. Baek, M. & Mann, R.S. Lineage and birth date specify motor neuron targeting and dendritic architecture in adult *Dorosphila*. *J. Neurosci.* **29**, 6904-16 (2009)

36. Jefferis, G.S., Marin, E.C., Stocker, R.F. & Luo, L. Target neuron prespecification in the olfactory map of Drosophila. *Nature* **414**, 204-8 (2001)

37. Espinosa, J.S. & Luo, L. Timing neurogenesis and differentiation: insights from quantitative clonal analyses of cerebellar granule cells. *J. Neurosci.* **28**, 2301-12 (2008)

38. Henze, D.A., Wittner, L. & Buzsaki, G. Single granule cells reliably discharge targets in the hippocampal CA3 network in vivo. *Nat. Neurosci.* **5**, 790-795 (2002)

39. Pinaud, R. *et al*, Detection of two mRNA species at single-cell resolution by double-fluorescence *in situ* hybridization. *Nat. Protocols* **3**, 1370-79 (2008)

40. Emmenlauer, M. *et al.* XuvTools: free, fast and reliable stitching of large 3D datasets. *J. Microscop.* **233**, 42-60 (2009)

41. Noctor, S.C., Martínez-Cerdeño, V., Ivic, L. & Kriegstein, A. R. Cortical neurons arise in symmetric and asymmetric division zones and migrate through specific phases. *Nat. Neuroscience* **7**, 136-44 (2004)

42. Gogolla, N., Galimberti, I., DePaola, V. & Caroni, P. Preparation of organotypic slice cultures for long term live imaging. *Nat. Protocols* **1**, 1223-26 (2006)

End notes

Supplementary information includes 12 supplementary figures and their legends. Supplementary Fig. 1 provides a summary of the main findings in the study.

We thank S. Arber, A. Lüthi and B. Roska (FMI) for critical comments on the manuscript. We are grateful to Aaron Ponti (FMI) for valuable data analysis assistance. The Friedrich Miescher Institut is part of the Novartis Research Foundation.

Author contributions: YD conceived and carried out the gene expression and the adult subpopulation mapping analysis; FD conceived and carried out the neurogenesis and synaptogenesis analysis; IG conceived and carried out the connectivity analysis; EC carried out and optimized the few cell genomics experiments; PC helped devise the experiments and wrote the manuscript.

The authors have no competing financial interests in the work.

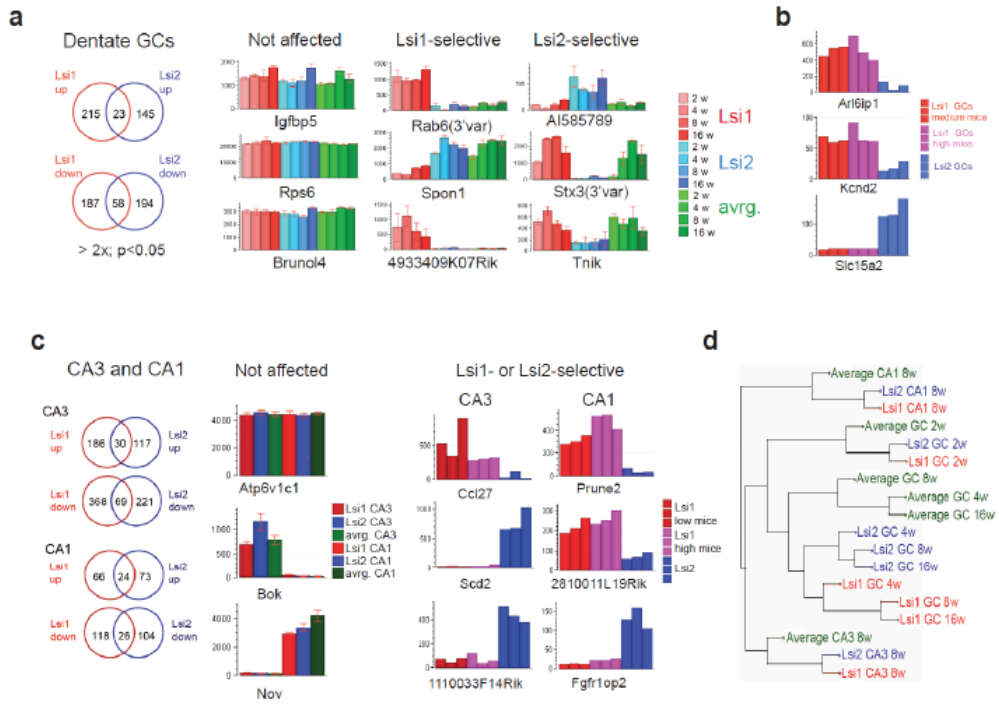

Figure 1

Distinct transcriptomes of Lsi1 and Lsi2 hippocampal principal neurons.

(a) Transcriptomes of Lsi1 and Lsi2 GCs. Left: numbers of genes up- or down-regulated compared to average (16 weeks data). Right: columns are average values from 3 mice.

(b) Comparable gene expression profiles in GCs from mice with many (15-20% of total) or few (2-5% of total) GFP-positive neurons. Columns are values in one mouse each.

(c) Transcriptomes of Lsi1 and Lsi2 pyramidal neurons. Details like in (a, b).

(d) In silico cell grouping. The unbiased hierarchical tree algorithm grouped cells according to subpopulations of GCs, and pyramidal neurons in CA3 an CA1.

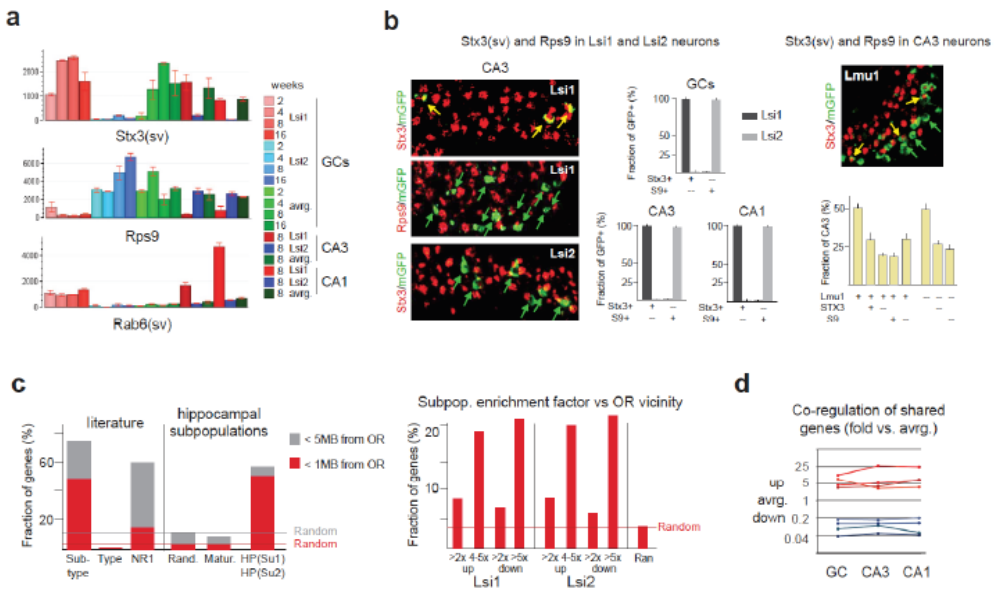

Figure 2

Identification of matched HP(Su1) and HP(Su2) subpopulations.

(a) Examples of transcripts co-regulated in Lsi1 or Lsi2 principal neurons in DG, CA3 and CA1.

(b) Marker combinations identifying Lsi1 and Lsi2 principal neurons in the hippocampus. Combined GFP/in situ hybridization detection. Arrows: GFP+/marker+ (yellow) and GFP+/marker- (green). Quantitative analyses: data from 8 sections each, covering all anterior-posterior levels of hippocampus; N=3 mice each. Right: distribution of STX3(sv) and Rps9 transcripts among pyramidal neurons in CA3.

(c) High probability for subtype specific genes to map near OR clusters. Left: relationship between subtype markers and OR cluster vicinity. Random: 400 random genes in average GCs; Maturation: genes enriched in Lsi1 (16w) over Lsi1 (8w) GCs; HP(Su1), HP(Su2): genes selectively regulated in all Lsi1 or Lsi2 principal neurons. Right: optimization of OR vicinity for genes up- (4-5 fold) or down-regulated (>5 fold) in Lsi1 or Lsi2 principal neurons.

(d) Genes up- or down-regulated in all three types of Lsi1 hippocampal principal neurons are closely co-regulated in GCs, and in pyramidal neurons in CA3 and CA1. Each line represents one gene, and its deviation from average values.

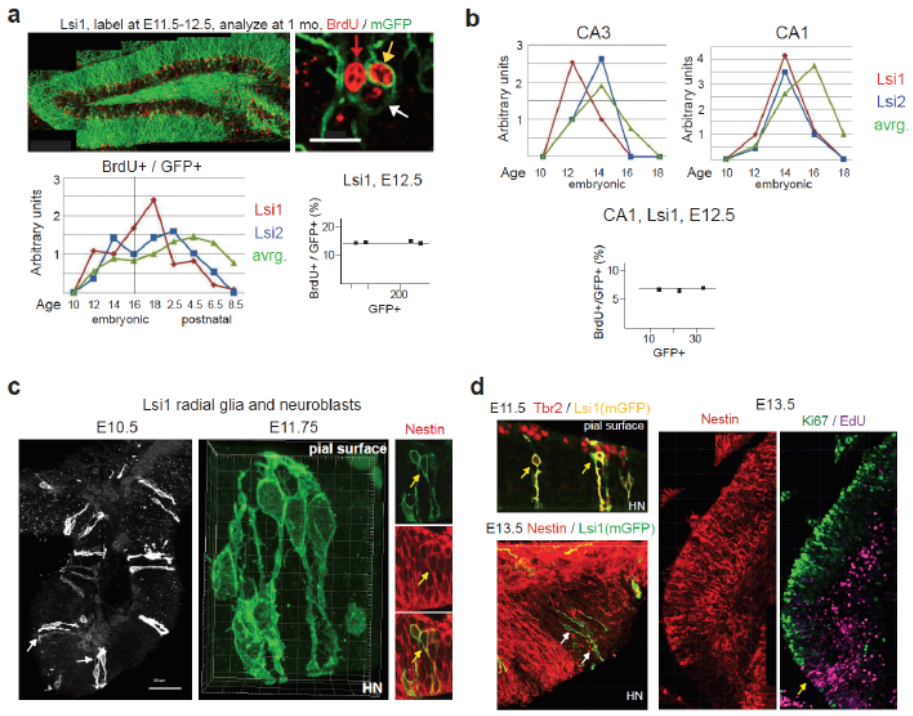

Figure 3

Specification of Lsi1 and Lsi2 principal neurons during hippocampal neurogenesis.

(a) Lsi1 and Lsi2 GCs are generated during early phases of neurogenesis. Top: BrdU labeling experiment; arrows: BrdU+/GFP+ GC (yellow), BrdU+/GFP- GC (red) and weakly BrdU+ GC (white). Lower panels, left: fractions of total GFP+ GCs labeled with BrdU at different time intervals (avrg.: fractions of all GCs labeled with BrdU). Averages from 3 mice each; values normalized to throughs between two neurogenesis peaks; vertical line: through between early and late neurogenesis wave for average GCs. Right panel: fractions of BrdU+/GFP+ neurons are not affected by total numbers of GFP+ GCs.

(b) Neurogenesis of Lsi1 and Lsi2 hippocampal pyramidal neurons. Details as in (a).

(c) Transgene expression during hippocampal neurogenesis. Expression in radial glia cells (left) and neuroblast groups (right). Some of the GFP+ neuroblasts are Nestin+ (right, arrow).

(d) Specification of Lsi1 neuroblasts during hippocampal neurogenesis. At E11.5, GFP+ neuroblasts (arrows) co-distribute with regions of proliferating precursors (Tbr2+; top, right). At E13.5, GFP+ neuroblasts (white arrows) accumulate in defined Ki67-depleted non-proliferating regions (N=6) that had been labeled with EdU at E11.5 (arrow), and are now depleted of Nestin precursors (arrow).

Bar: 20 µm.

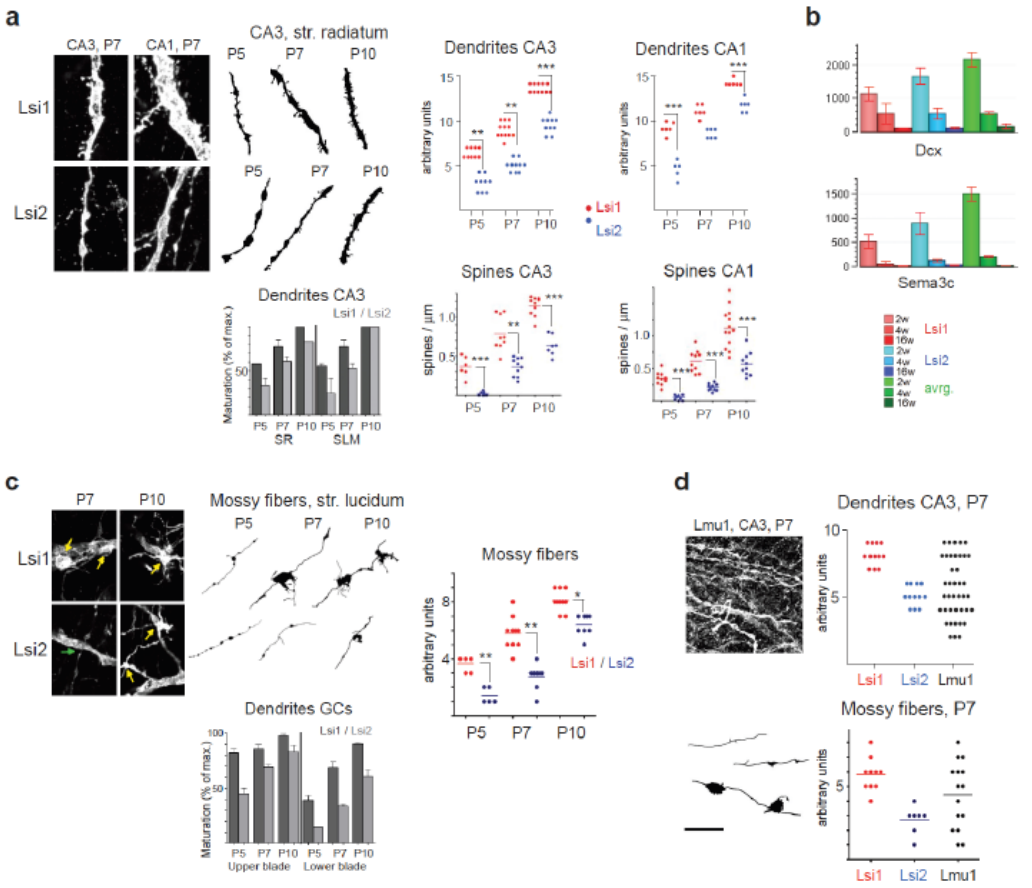

Figure 4

Distinct synaptogenesis schedules of HP(Su1) and HP(Su2) subpopulations.

(a) Non-overlapping dendritic maturation and synaptogenesis processes in Lsi1 and Lsi2 pyramidal neurons in CA3 and CA1. Left and center: representative panels and camera lucidas. *, **, **: $p<0.05$, $p<0.01$, $p<0.001$.

(b) Immature GC transcript contents in Lsi1, Lsi2 and average GCs. Dcx: Doublecortin.

(c) Non-overlapping dendritic maturation and synaptogenesis processes by Lsi1 and Lsi2 GCs. Arrows: presence (yellow) or absence (green) of specific contacts between mossy fibers and pyramidal neurons. Scatter plot: presynaptic maturation index values.

(d) Synaptogenesis subgroups within Lmu1 pyramidal neurons and mossy fibers at P7. Panel and camera lucida: representative examples of labeled dendrites (panel, stratum radiatum) and mossy fibers (lucida). Bar: 10 µm.

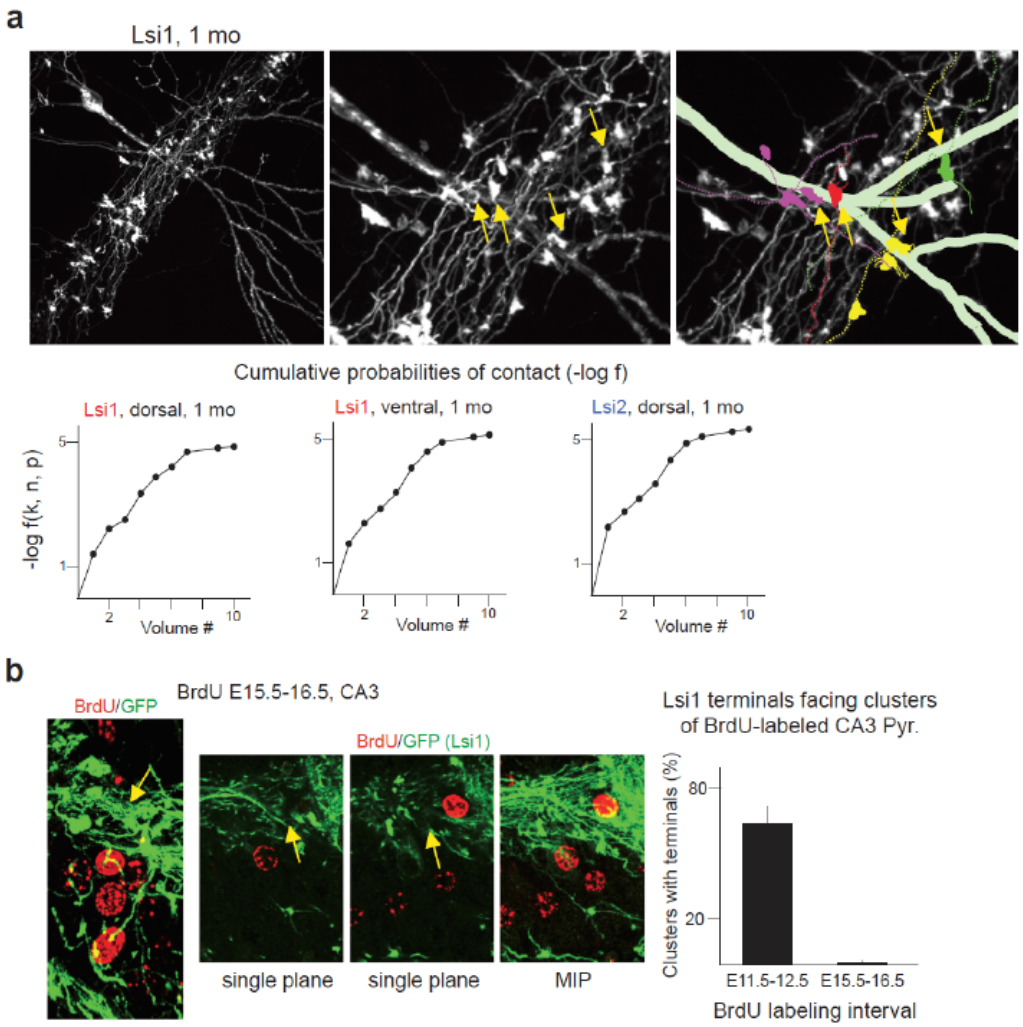

Figure 5

Selective connectivity between matched GCs and CA3 pyramidal neuron subpopulations.

(a) Analysis of stratum lucidum synapses in Lsi1 and Lsi2 mice. The panels show examples of verified contacts (yellow arrows) in Lsi1 mice at one month. Quantitative analysis: cumulative probability values for first 10 volumes (averages from 3 mice each).

(b) Lsi1 mossy fibers establish synapses facing clusters of early- but not late-born pyramidal neurons. Panels: examples from 1 mo Lsi1 mouse labeled with BrdU at E15.5-16.5 (late-born pyramidal neurons). Yellow arrows: Lsi1 mossy fiber stretch facing BrdU+ neurons, and devoid of mossy fiber terminals (white arrows). Quantitative analysis: 30 clusters each, from 3 mice.

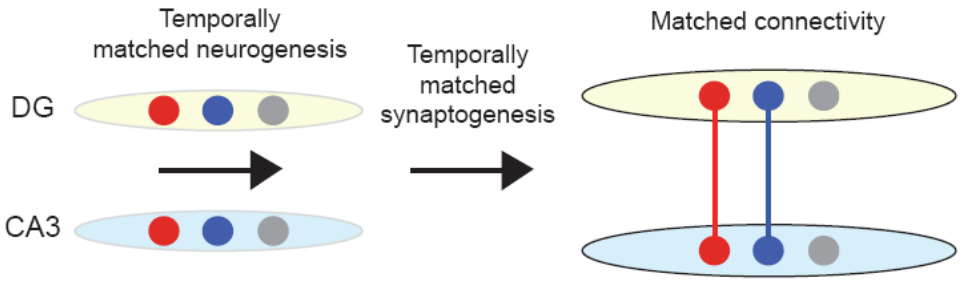

Supplementary Fig. 1

Schematic of main findings.

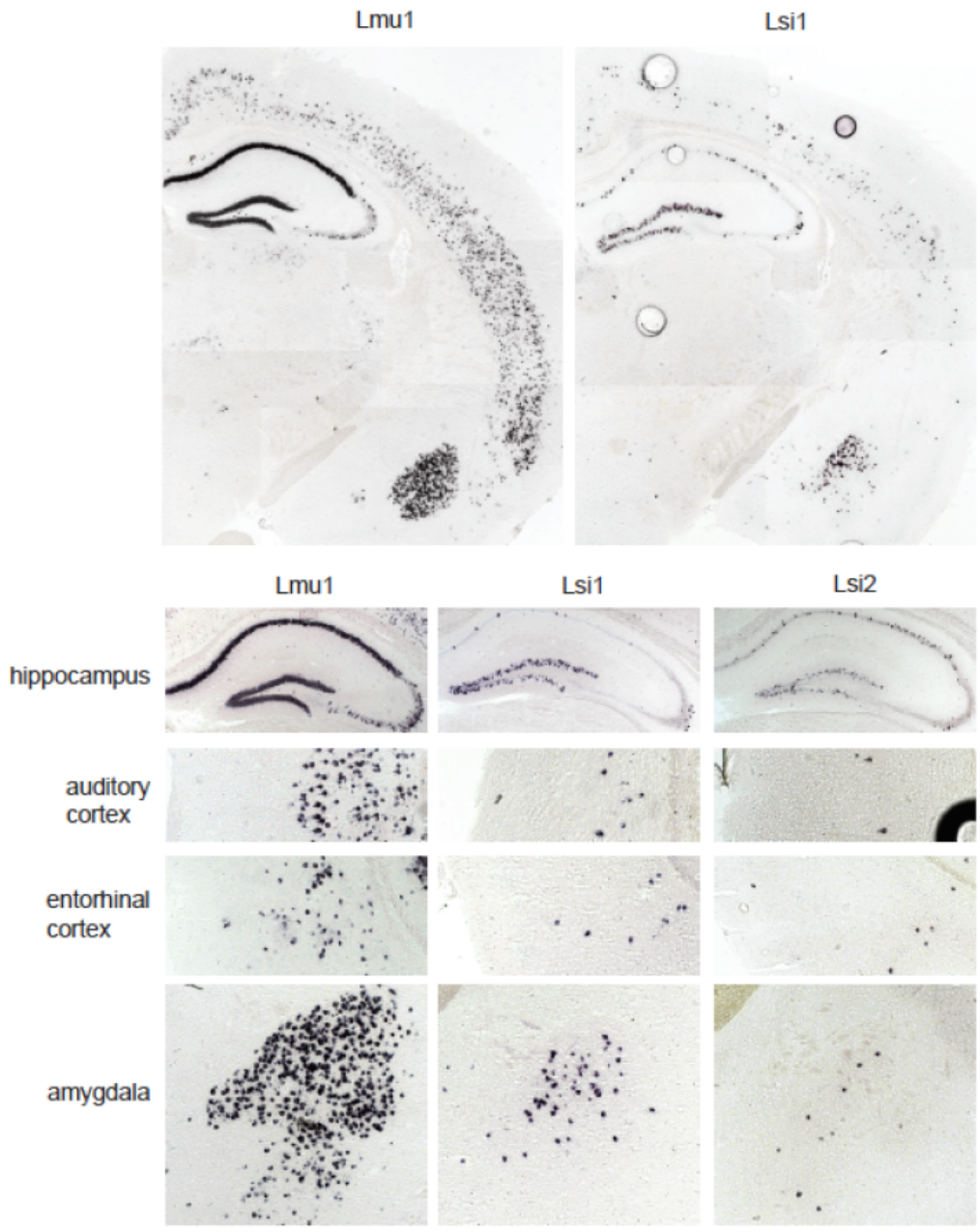

Supplementary Fig. 2

Distribution of transgene-positive cells in Lmu1, Lsi1 and Lsi2 mice.

In situ hybridization in 2 mo mice. Note how positive neurons are detected in the same structures but in different numbers in Lmu1, Lsi1 and Lsi2 mice.

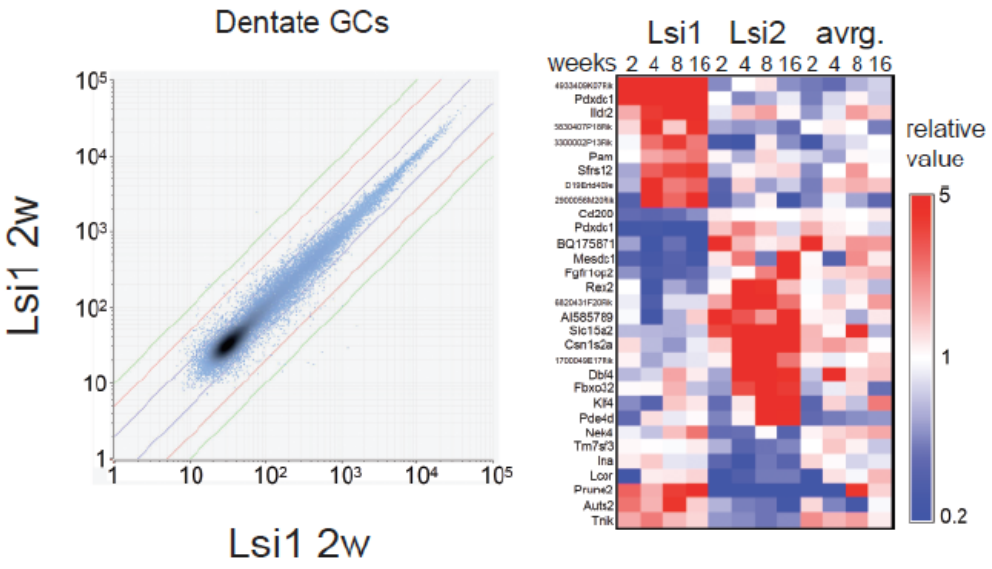

Supplementary Fig. 3

Distinct transcriptomes of Lsi1 and Lsi2 hippocampal GCs.

Left: reproducibility of microarray analysis. Right: heat map for 30 differentially regulated genes at 4 different ages.

Lsi1 vs. avrg. GC 16w >5X

Lsi1/avrg.		Lsi1/avrg.	
BG074974	21.9	B130021B11Rik	0.03
Trip11	16.5	Lpl	0.04
Ptprd	14.9	Skiv2l	0.04
Zc3hav1	14.0	Kcnj9	0.05
Rhobtb1	13.6	BE943757	0.06
Snx6	13.1	Smpd4	0.06
Zc3h8	11.9	9330169B04Rik	0.06
Pdxdc1-sv1 (NM_053181.1)	11.6	BB024203	0.07
		BQ175871	0.08
BB473548	11.5	BB188453	0.08
Cnot6l	11.3	Rps9	0.08
Auts2	11.0	Slco4a1	0.08
Csn2	10.5	Vti1a	0.08
Dgkd	10.2	Cldnd1	0.08
Ssrp1	9.5	Gpc6	0.09
Rsrc1	8.5	Slc39a8	0.09
A930018M24Rik	8.4	Bcat1	0.09
5830407P18Rik	8.2	Kirrel3	0.09
Btbd9	8.2	Mapk10	0.10
Rpl17	7.7	D9Ertd306e	0.10
Lrp1b	7.2	Pcdh15	0.10
Mapk10	7.1	Sox11	0.10
5830469G19Rik	6.7	Tsc22d1	0.11
Gabrb3	6.6	Lrch1	0.12
Evi5	6.5	4732496C08Rik	0.12
Lhx9	6.0	Arid5b	0.12
B230334C09Rik	5.8	Thumpd1	0.12
Schip1	5.7	BB725777	0.13
Ddx6	5.6	Pou4f2	0.13
Srp54a	5.5	Dnm3	0.13
C730049O14Rik	5.5	Serpina3n	0.14
Vav3	5.5	BQ266161	0.14
BF472132	5.3	Wwtr1	0.14
Lpin1	5.2	Agl	0.15
Foxn2	5.2	5830426K05Rik	0.15
D3Ertd254e	5.2	Phip	0.16
Trip12	5.1	BG067986	0.17
Cops2	5.0	C130015C19	0.17
		Zfp398	0.17
		Zbtb25	0.18
		Pdxdc1-sv2 (NM_001039533)	0.18
		BB163080	0.18
		Agtg2	0.19
		AV233159	0.19
		Iffo2	0.20
		AW554842	0.20

Lsi2 vs. avrg. GC 16w >5X

Lsi2/evrg.		Lsi2/avrg.	
4930445G23Rik	19.1	Kirrel3	0.01
Rbm39	15.6	Prune2	0.04
Ptprd	11.6	Kcnj9	0.04
9430085L16Rik	11.5	Skiv2l	0.04
Setd4	11.2	Gpc6	0.07
BB183349	10.1	Btrc	0.08
5830469G19Rik	9.8	BB354702	0.08
Ltbp1	9.6	Stx3 -sv1 (NM_011502)	0.08
BM213120	9.6		
BB548287	9.2	Lnpep	0.09
Trip11	9.1	Cldnd1	0.10
Rpl17	8.5	Btbd11	0.10
Chm	8.5	Tmem29	0.10
B230114P17Rik	8.4	Fam76b	0.11
Fbxo32	8.3	Lpl	0.11
Mmm2	8.3	Eftud2	0.12
2610301B20Rik	8.1	Nsun6	0.12
Mef2c	7.8	Zfp398	0.12
BB180869	7.8	Zw10	0.12
5730510P18Rik	7.8	BB221878	0.12
Ttn	7.6	AK136898	0.13
Nav2	7.3	Mapk10	0.13
Slc15a2	7.2	BB750374	0.13
Rbm39	6.7	Ap3s2	0.13
BB251113	6.0	2410085M17Rik	0.13
Rhobtb1	6.0	Timm44	0.13
6030400A10Rik	5.9	C80889	0.14
C79246	5.8	Ncor1	0.14
Srd5a3	5.8	Map2k5	0.14
Bicd1	5.7	Tax1bp1	0.14
Ccni	5.7	C77673	0.14
Ly86	5.5	Tmem41b	0.14
5330423I11Rik	5.5	AI120166	0.15
Cd24a	5.1	5730470L24Rik	0.15
Iif3	5.0	Ggps1	0.15
		Lphn2	0.16
		Rb1	0.16
		Eno1	0.16
		Kcnc2	0.16
		Pcdha4	0.17
		D5Ertd798e	0.17
		Nfatc3	0.17
		Ankhd1	0.17
		BB461843	0.18
		2310008H04Rik	0.18
		Tgfbr3	0.18
		BC043301	0.19
		Serpina3n	0.19
		Zfp148	0.19
		Igf2r	0.19
		BC021831.1	0.19

Lsi1 vs. Lsi2 GC 16w >5X

Lsi1/Lsi2	
Prune2	97.8
2900056M20Rik	31.6
Snx6	17.2
BB473548	16.6
Stx3 -sv1 (NM_011502)	14.4
Zc3h8	13.9
Tgfbr3	13.5
2900017F05Rik	13.2
Mkln1	12.0
Tpd52l2	11.6
Zw10	10.7
Pdxdc1-sv1 (NM_053181.1)	10.4
Zfp697	9.9
Btrc	9.7
Acap2	9.2
Asxl3	9.1
5830407P18Rik	9.0
5730470L24Rik	9.0
Ggps1	8.8
Auts2	8.2
Kirrel3	7.9
6330526H18Rik	7.8
Pds5a	7.8
Spab2	7.5
BB040234	7.2
Rab6-sv1 (BC019118)	7.0
Auts2	6.9
Arl6ip1	6.8
E430022K19Rik	6.8
BB221076	6.8
Zbtb20	6.7
Tmem109	6.6
BF472132	6.3
Rbm39	6.2
B230334C09Rik	6.2
Btbd9	6.1
9430047L24Rik	6.0
Tra2b	5.8
Srp54a	5.8
E430028B21Rik	5.8
Elovl7	5.8
Rb1cc1	5.7
Mapk6	5.7
BB126857	5.6
Fam76b	5.4
Trip12	5.4
D5Wsu178e	5.3
3300002P13Rik	5.1

Lsi2/Lsi1	
Rps9	26.9
BE943757	26.1
Mesdc1	20.5
Fgfr1op2	15.0
Lrch1	10.2
C130015C19	10.0
AU014972	9.9
2610301B20Rik	9.8
BB075068	9.3
Thumpd1	9.3
Arap3	8.7
Svil	8.6
Mmm2	8.5
Col6a2	8.5
Csn1s2a	8.4
BQ175871	8.4
Ttn	7.6
AI450353	7.4
Slc20a2	7.4
Ccni	6.9
D14Ertd725e	6.7
Slc15a2	6.5
Nrf1	6.2
Zfp383	6.1
Klf4	6.1
Pdgfc	6.0
C80279	5.8
Pdxdc1-sv2 (NM_001039533)	5.6
BE134355	5.6
Hbs1l	5.6
Kctd9	5.5
Fbxo32	5.5
1810043G02Rik	5.5
Srd5a3	5.4
Ube2w	5.4
Urm1	5.1
Tcfap4	5.0

Supplementary Fig. 4

Genes up- or downregulated in Lsi1 or Lsi2 granule cells. Values are averages from 3 mice (16 weeks).

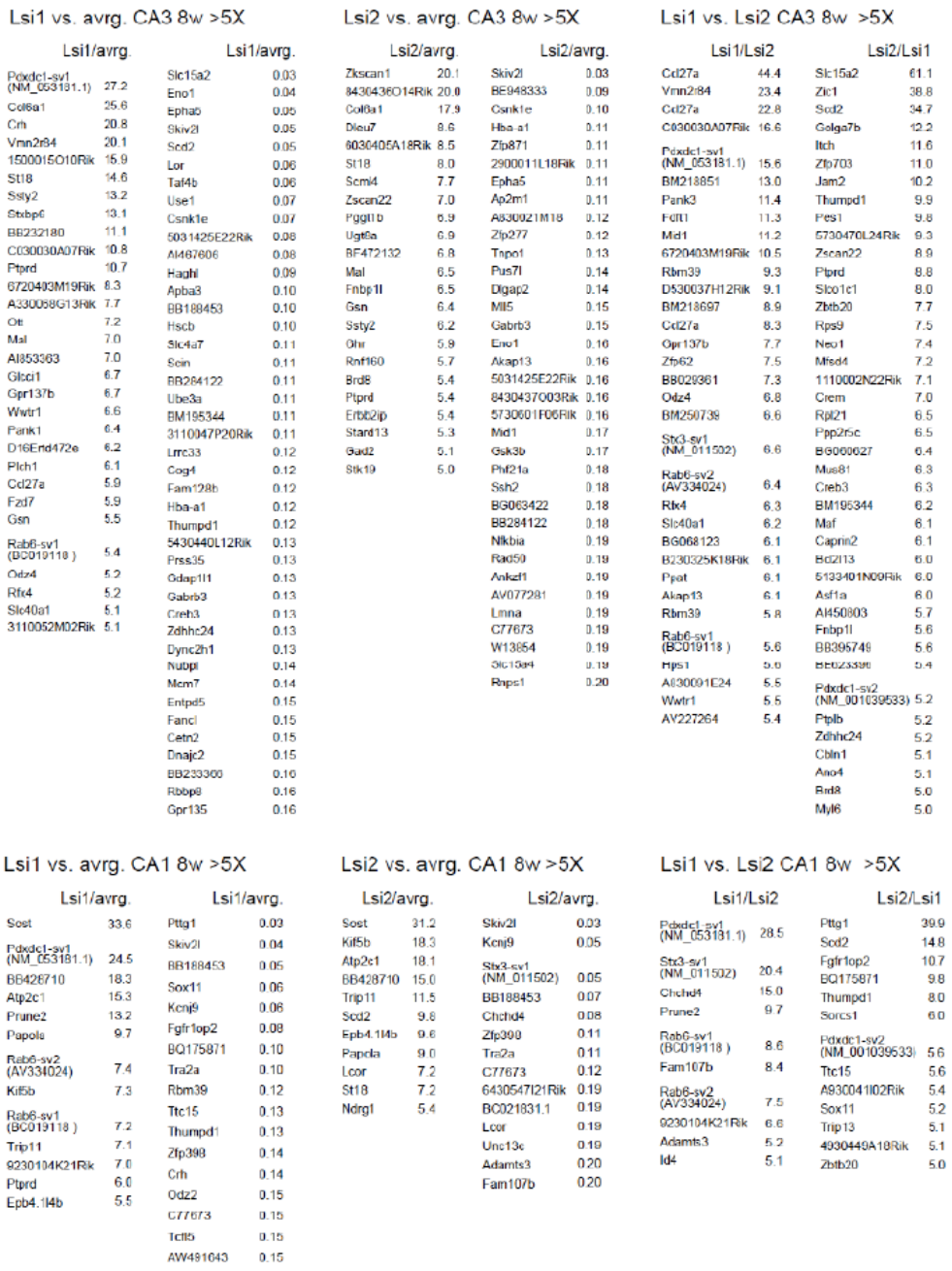

Supplementary Fig. 5

Genes up- or downregulated in Lsi1 or Lsi2 CA3 or CA1 pyramidal neurons. Values are averages from 3 mice (16 weeks).

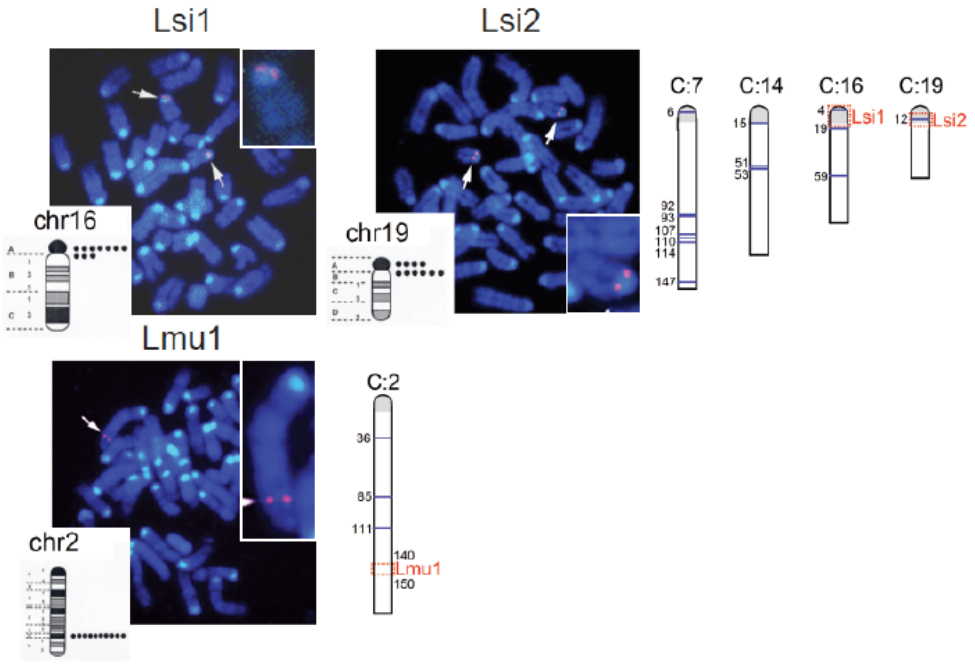

Supplementary Fig. 6

Visualization of transgene insertion sites by FISH. The positions of OR clusters are indicated by bars and numbers on the chromosome schematics on the right. The insertion sites for Lsi1 and Lsi2 mice are near centromeres, on two of the four mouse chromosomes with OR clusters near centromeres (C7, C14, C16, C19).

Subtype genes)

retinal neuron subtype genes

	Mm	Hs
Grm6	0.1	2.4
Prkca	0.3	8.5
Rho	0.5	0.5
Fstl4-Spig1	0.6	>15
Slc6a9-Glyt1	0.8	>15
Scube2	0.9	1.1
Gjd2-Cx36	1.8	>15
Th	2.2	2.1
Pde1b	5	0.6
Gjc1-Cx45	5.8	13.6
Cabp5	7.5 *	>15
Aqp1	12.1**	>15
Chat	17.3	5.4

* 0.2 form vomeronasal 1 receptor
** 1.6 form vomeronasal 1 receptor

DRG subtype genes

	Mm	Hs
Trpv1	0.1	0.2
P2rx3-p2x3	0.3	0.5
Prph	0.6	0.7
Ret- c-RET	1.6	2.2
Mrgprd	4.6	1
Calca-Cgrp	5.8	0
Ntrk1-TrkA	9.6	1.5

cerebellum subtype genes

	Mm	Hs
Nrgn	0.1	0.2
Gst	4.2	>15
Aldoc-Zebrin2	4.1	>15

cell type genes)

broader retinal cell type genes

	Mm	Hs
Dab1	14	>15
Cnga3	57.2	>15
Slc17a8-vGlut3	10.5	>15
Gja10-Cx-57	11	>15
Calb2	24.9	>15
Calb1	27.9	no OR
Opn4	15.1	>15

broad interneuron marker genes

	Mm	Hs
Pvalb	20	no OR
Chat	17.2	5.4
Gad2-GAD65	13.7	>15
Gad1-GAD67	14.8	>15

cerebellar Golgi cell type marker

	Mm	Hs
Grm2	66.7	>15

motor neuron marker

	Mm	Hs
Mnx1-HB9	no OR	12.5

Lsi1 co-regulated genes all DG+CA3+CA1 more than 3 fold

	DG	CA3	CA1	Mm	Hs
Pdxdc1-sv1 (NM_053181.1)	11.6	27.2	24.5	5.4	11.8
Rab6-sv1 (BC019118)	4.3	5.4	7.2	0.9	1.4
Rpl17	7.7	3.1	3.5	0.8	>15
Rab6-sv2 (AV334024)	3.4	3.9	7.4	0.9	1.4
BB188453	0.08	0.10	0.05	0.2	-
Skiv2l	0.04	0.05	0.04	1.6	2.5
Pdxdc1-sv2 (NM_001039533)	0.18	0.17	0.20	5.4	11.8
Thumpd1	0.12	0.12	0.13	10.9	>15

Lsi2 co-regulated genes all DG+CA3+CA1 more than 3 fold

	DG	CA3	CA1	Mm	Hs
Stx3-sv1 (NM_011502)	0.08	0.23	0.05	0	0
C77673	0.14	0.19	0.12	6.5	-

Lsi1 or Lsi2 co-regulated genes in 2 regions more than 3 fold

	Mm	Hs
Zfp398	4.6	4.9
Rps9	0.7	16*
Kcnj9	0.7	>15*
Spon1	4.9	6.2
Sost	6.7	14.4
Eftud2	5.8	13.3

* There is an immunoglobulin gene less than 0.1 million bp.

Supplementary Fig. 7

Subtype-specific genes and shared matched subpopulation genes have a high probability to map near OR clusters. Subtype genes: all known retinal neuron markers, and all DRG markers. Cell type markers: known general retinal and interneuron markers. Mm: mus musculus; Hs: homo sapiens.

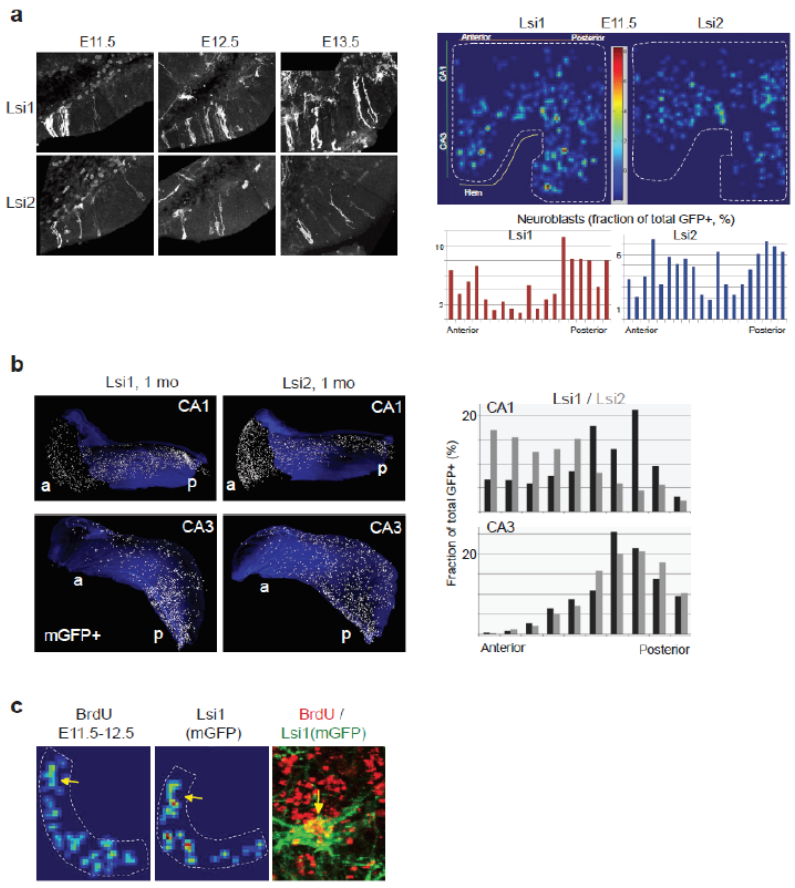

Supplementary Fig. 8

Specification of Lsi1 and Lsi2 principal neurons during hippocampal neurogenesis and comparison to distributions in adult hippocampus.

(a) Left: representative patterns of GFP+ neuroblast distributions in HN of Lsi1 and Lsi2 embryos (Hem to the left). Right: Spatial distribution of GFP+ neuroblasts in HN of Lsi1 and Lsi2 embryos at E11.5. The heat map (top) visualizes specific differences between Lsi1 and Lsi2 embryos at the same developmental age; the quantitative analysis (bottom) represents average values for 3 embryos each.

(b) Patterns of Lsi1 and Lsi2 pyramidal neurons in the adult hippocampus. Left: representative 3D-maps of GFP+ pyramidal neurons (white dots) throughout CA1 and CA3. Right: quantitative analysis of the distributions. Median values from 3 mice each; note resemblance to distributions in HN (a).

(c) Comparable distributions of early (E11.5-12.5) BrdU-labeled and GFP+ Lsi1 pyramidal neurons (e.g. arrows). Heat map data from 1 mo mouse. Panel on the right: cluster of BrdU+/GFP+ pyramidal neurons in CA3 (arrow).

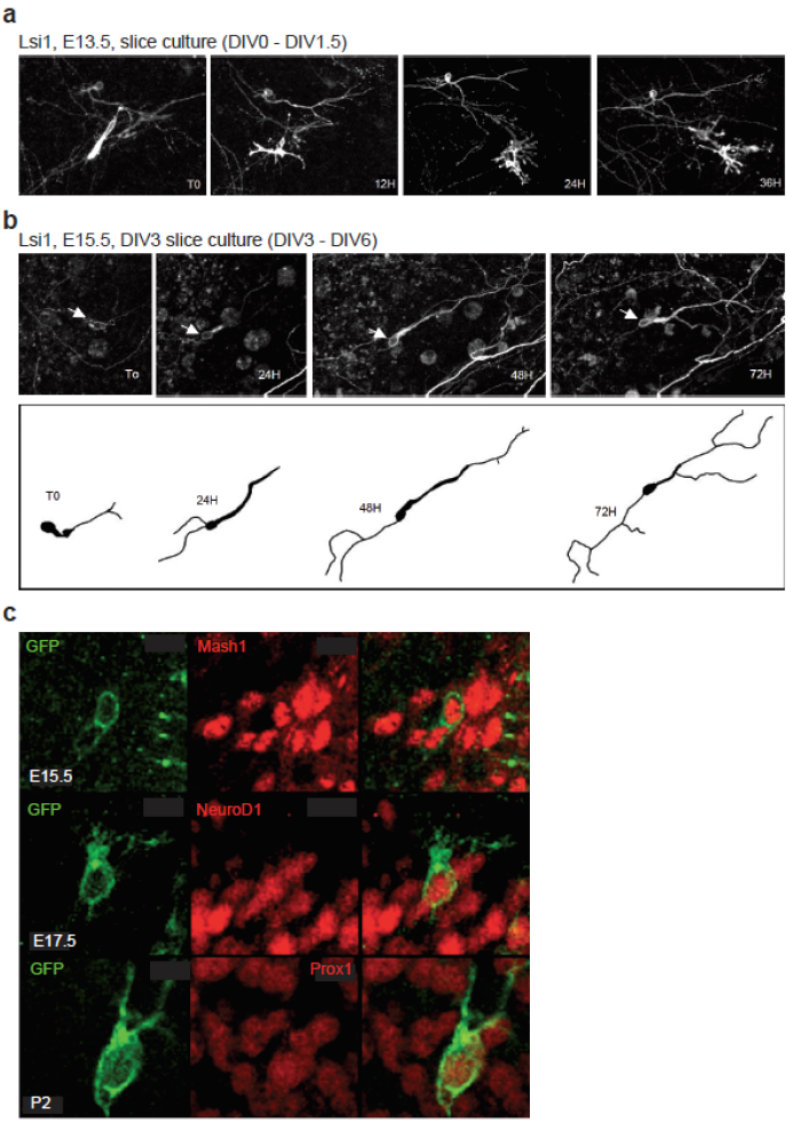

Supplementary Fig. 9

Maturation of GFP-positive Lsi1 neuroblasts.

(a) Time lapse imaging of Lsi1 E13.5 slice culture. Neuroepithelium on the right. Note mitotic division of Lsi1 neuroblast to generate GFP+ Lsi1 daughter cells.

(b) Time lapse imaging of DIV3 Lsi1 E15.5 slice culture. The camera lucida highlights a neuroblast that develops dendritic and axonal primordia between DIV3 and DIV6.

(c) Maturation of mGFP-positive neuroblasts *in vivo*. Immunocytochemistry panels visualize mGFP+ cells co-expressing Mash1 (E15.5; early progenitors), NeuroD1 (E17.5; postmitotic neuroblasts) and Prox1 (P2; immature granule cells).

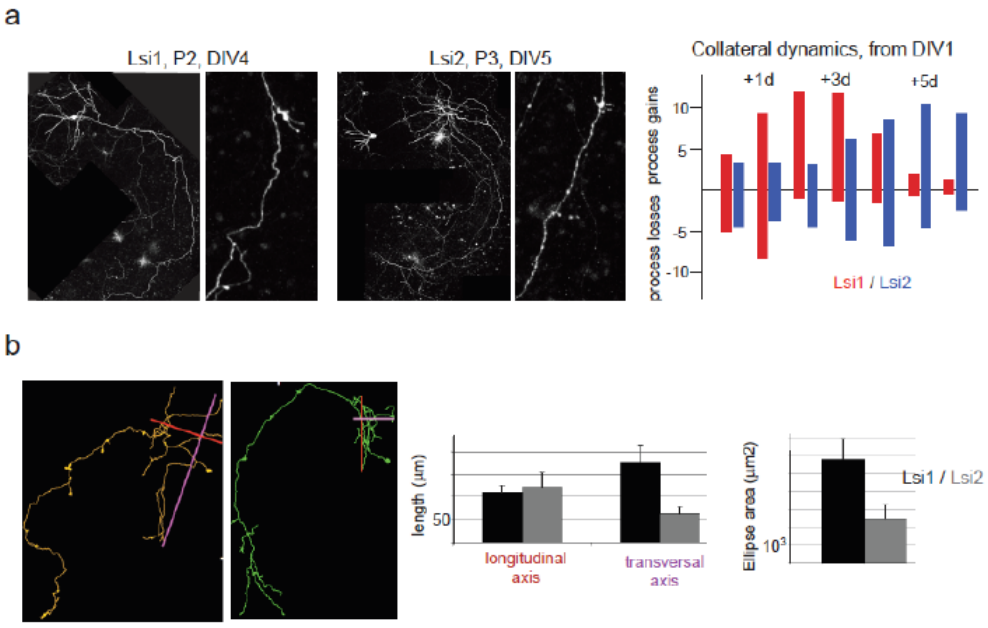

Supplementary Fig. 10

Distinct mossy fiber properties by Lsi1 and Lsi2 GCs *in vitro* and *in vivo*.

(a) Mossy fiber maturation *in vitro*. Panels: examples of comparable mossy fiber maturation stages in P2 + 4DIV Lsi1 and P3 + DIV5 Lsi2 slice cultures. The quantitative analysis is based on time lapse imaging of Lsi1-P2 and Lsi2-P3 cultures, from DIV1 on. Numbers of collaterals per mossy fiber that will have grown (process gains) or shrunk (process losses) one day later. Synaptogenesis coincides with a phase of increased collateral dynamics; it is maximal from days +1 to +3 in Lsi1 mossy fibers, and from days +3 to +6 in Lsi2 mossy fibers. Averages from 4 mossy fibers each.

(b) Distinct hilar collateral arborizations in Lsi1 and Lsi2 mossy fibers *in vivo*. Camera lucidas: illustration of longitudinal and transversal hilus collateral axes for a Lsi1 and a Lsi2 GC at 1 mo. Longitudinal axis: from cell body to beginning of CA3; transversal axis: longest extent of collateral extension perpendicular to longitudinal axis. Quantitative analysis: Lsi1 mossy fiber collaterals arborize through larger extent of hilus that their hilar counterparts. Ellipse areas were computed for individual mossy fibers, based on their longitudinal and transversal axes. N=20 each.

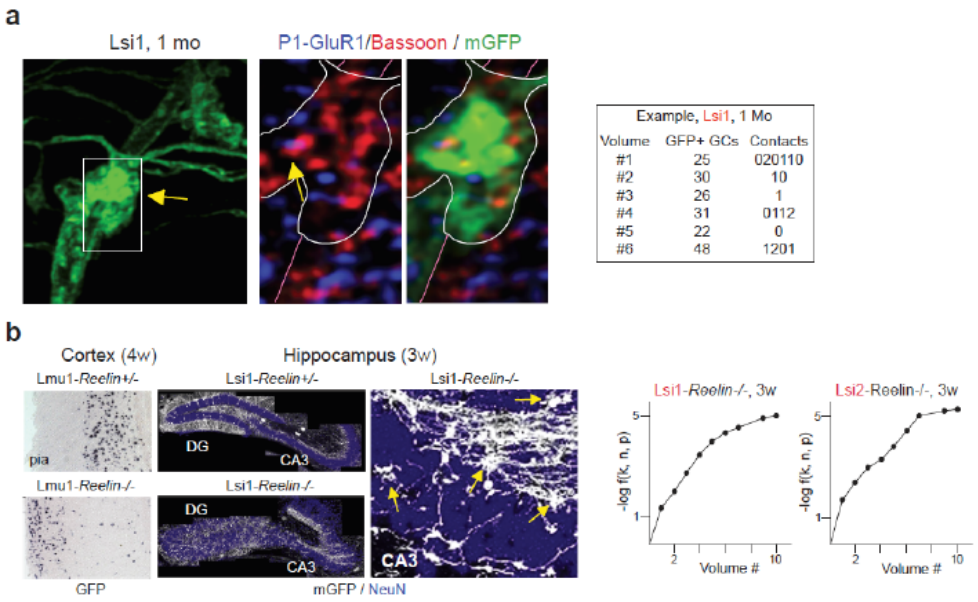

Supplementary Fig. 11

Selective connectivity between mossy fiber and CA3 pyramidal neuron subpopulations.

(a) Left: example of verified mossy fiber terminal/pyramidal neuron contact (yellow arrows) in Lsi1 mouse at one months. Lsi1 mossy fiber from left to right; Lsi1 pyramidal neuron dendrite from bottom left to top right. High-mag panels are single confocal planes. Right: example of quantitative analysis raw data for six individual volumes along CA3 in a 1 mo Lsi1 mouse. The values for „contacts“ are the number of mossy fiber terminals contacting individual Lsi1 pyramidal neurons inside that volume (e.g. six of them in volume #1).

(b) Selective connectivity between Lsi1 or Lsi2 subpopulations in the absence of Reelin. Left: Disruption of cortical organization in *Reelin-/-* mice: GFP+ Lmu1 neurons in layer 5 and 6 are displaced towards the pia in the absence of Reelin. Center: disruption of cell layering in the hippocampus, and clustering of Lsi1 mossy fiber terminals in CA3 (arrows) in the absence of Reelin. Right: selective stratum lucidum connectivity in Lsi- and Lsi2-*Reelin-/-* mice.

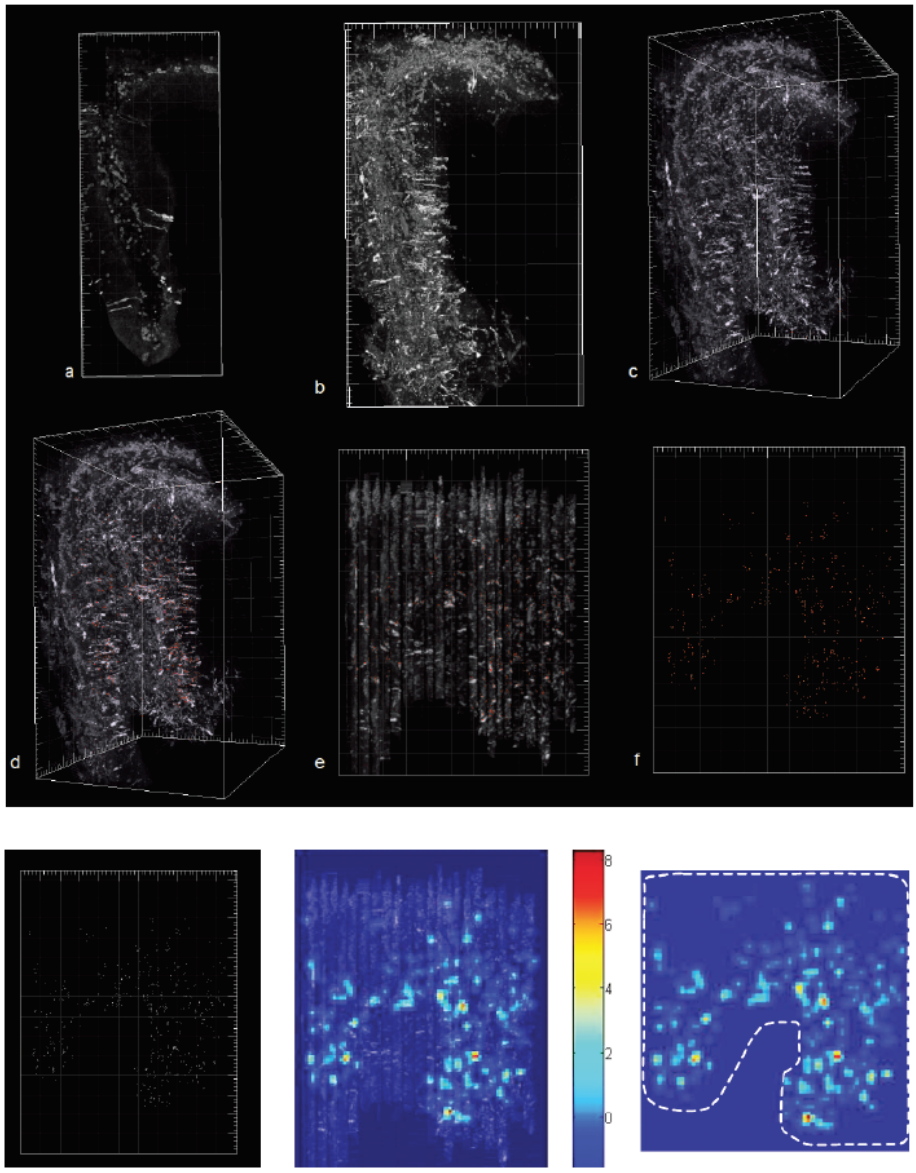

Supplementary Fig. 12

Heat map procedure to analyze the distribution of transgene-positive cells in an E11.5 Lsi1 embryo (Fig. 3b).

Upper panel: Workflow description for dataset acquisition. Confocal acquisition and 3D stiching (a; XuvTools); alignment at single plane level (b; Photoshop CS3); 3D reconstruction (c, Imaris); spot tracing (d); rotation and spot density analysis (Matlab).

Lower panels: Heat map generation based spot positioning procedure. A sliding window procedure (Matlab) based on local spot densities generates a heat map (center); background (revealing individual sections, center) is filtered, and HN outline is added (dotted line) to generate the final map on the right.

2.2 Additional data

This section contains further results and preliminary findings all concerning the subtypes of principal neurons in the hippocampus.

2.2.1 Distribution patterns of GFP-positive cells

It has been suggested that subregions in the hippocampus can be subdivided into molecular domains based on gene expression patterns (Thompson et al., 2008). The comprehensive 3D reconstructions of the distributions of GFP-positive cells in the hippocampus of Lsi1 or Lsi2 mice revealed that there GFP-positive cells were absent from some of the subdomains (Fig.1).

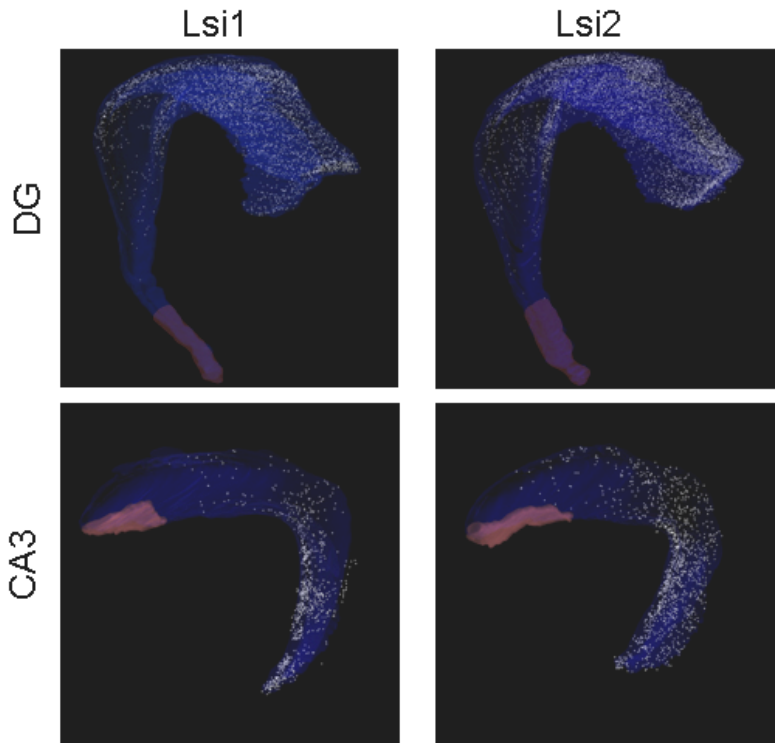

Figure 1. no GFP-positive cells in entire hippocampal subdomains.
white dot: GFP-positive cell, blue surface: outline of the dentate gyrus or CA3 pyramidal cell layer, red: particular molecular domains

We further determined whether GFP-positive cells in the Lsi1 or Lsi2 mice may be clustered in the adult. To address this question, a clustering program was used as analytical tool. In this program, if the distance between two cells is shorter than the threshold distance in 3D, these two cells are assigned the same color (Fig.2).

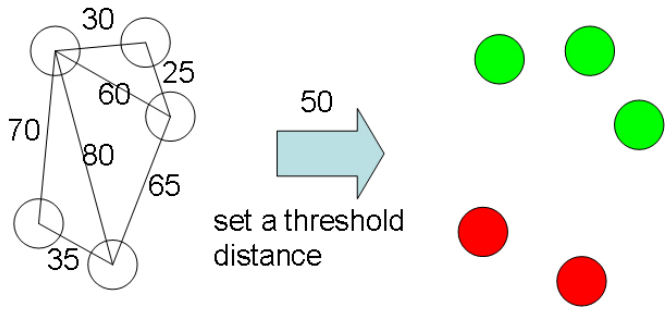

Figure 2. clustering program

More GFP-positive granule cells or CA3 pyramidal cells in Lsi1 or Lsi2 belonged to larger clusters than was obtained with a random distribution pattern for the same total number of cells (Fig.3).

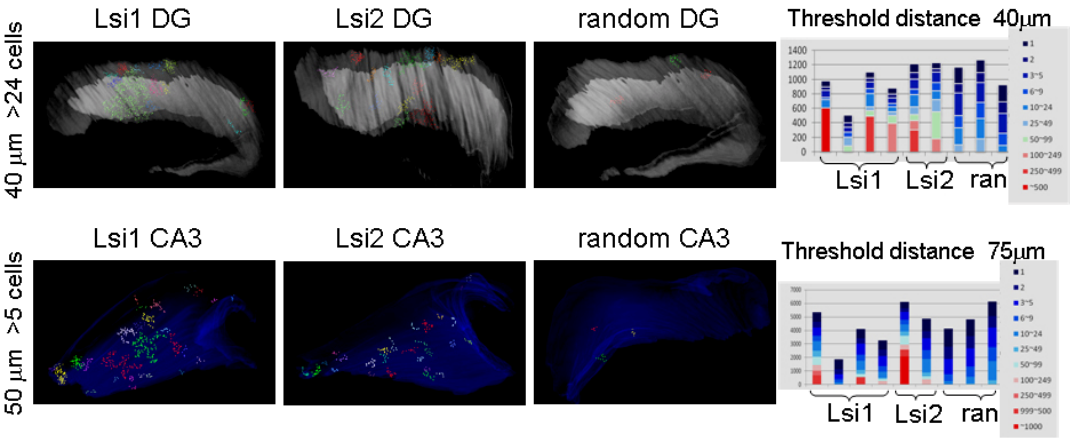

Figure 3. visualizing the clusters larger than a certain number
DG: The threshold was 40 μm. Clusters contained more than 24 cells were presented.
CA3: The threshold was 50 μm. Clusters contained more than 5 cells were presented.
The Y axis of the charts was the total number of the cells.

These results suggested that GFP-positive granule cells or CA3 pyramidal cells in Lsi1 or Lsi2 tend to be more clustered than would be predicted from a random distribution.

2.2.2 *The chromosomal location of the transgene in Lsi3 mice*

Another transgenic mouse line (Lsi3), which expresses GFP under the Thy1 promoter was generated in the laboratory of S. Arber. Granule cells in adult Lsi3 mice were sparsely labeled. The chromosomal location of the GFP construct in Lsi3 was identified by FISH. This revealed that the construct had also inserted in the vicinity of an OR gene cluster, although not in the vicinity of a centromere (Fig.4).

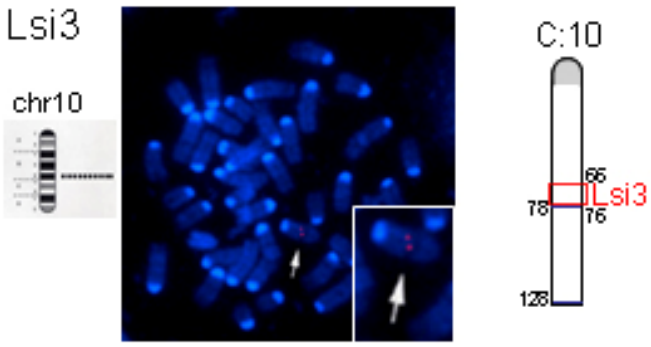

Figure 4. the chromosomal location of the construct in Lsi3
C: chromosome number, Blue bars and numbers on the left side: OR genes location, numbers on the right side: possible location range of the construct

This finding would be consistent with the possibility that the vicinity to an OR gene cluster plays a role in generating the sparse labeling patterns.

2.2.3 HDAC inhibitor treatment in hippocampal slice cultures

Chromatin modifications have a role in learning and memory (Fischer et al., 2007; Vecsey et al., 2007; Guan et al., 2009). For example, histone deacetylase (HDAC) inhibitors enhance memory and synaptic plasticity (Vecsey et al., 2007), and environmental enrichment induced hippocampal and cortical acetylation and methylation of histones 3 and 4 (Fischer et al., 2007).

To investigate whether chromatin modifications may influence the properties of hippocampal subpopulations, I analyzed trichostatin A (TSA)-treated hippocampal cultures.

When TSA was administered to the hippocampal slices from Lsi1 mice, the intensity of the GFP signal was increased in a reversible manner (Fig.5). By contrast, no GFP-negative neurons became GFP-positive during the TSA treatment.

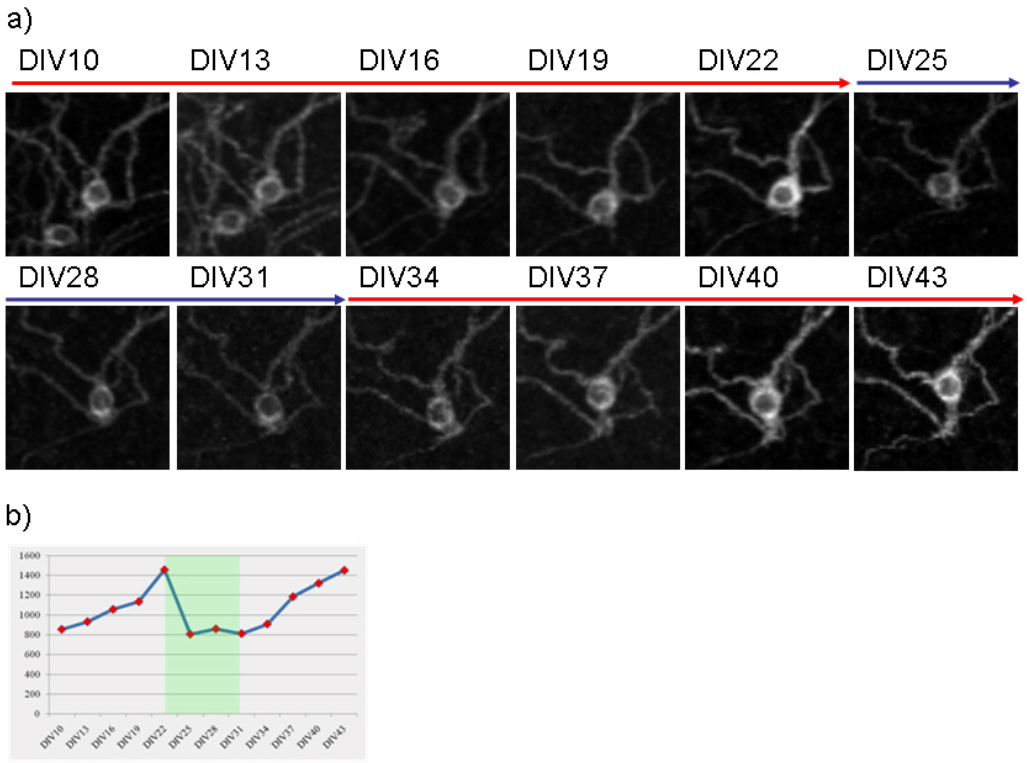

Figure 5. TSA changed the GFP intensity of Lsi1 positive granule cells in the slice culture
a) time-lapse imaging of Lsi1 GFP-positive granule cells in the hippocampal slice culture
red arrow: 500 nM TSA in culture medium, blue arrow: no TSA in culture medium
DIV: day in vitro
b) GFP intensity of a cell body, light green: No TSA in culture medium

Interestingly, the total volume of GFP-positive large mossy fiber terminals was reversibly increased by the TSA in Lsi1, but not in Lsi2 slice cultures. (Fig.6).

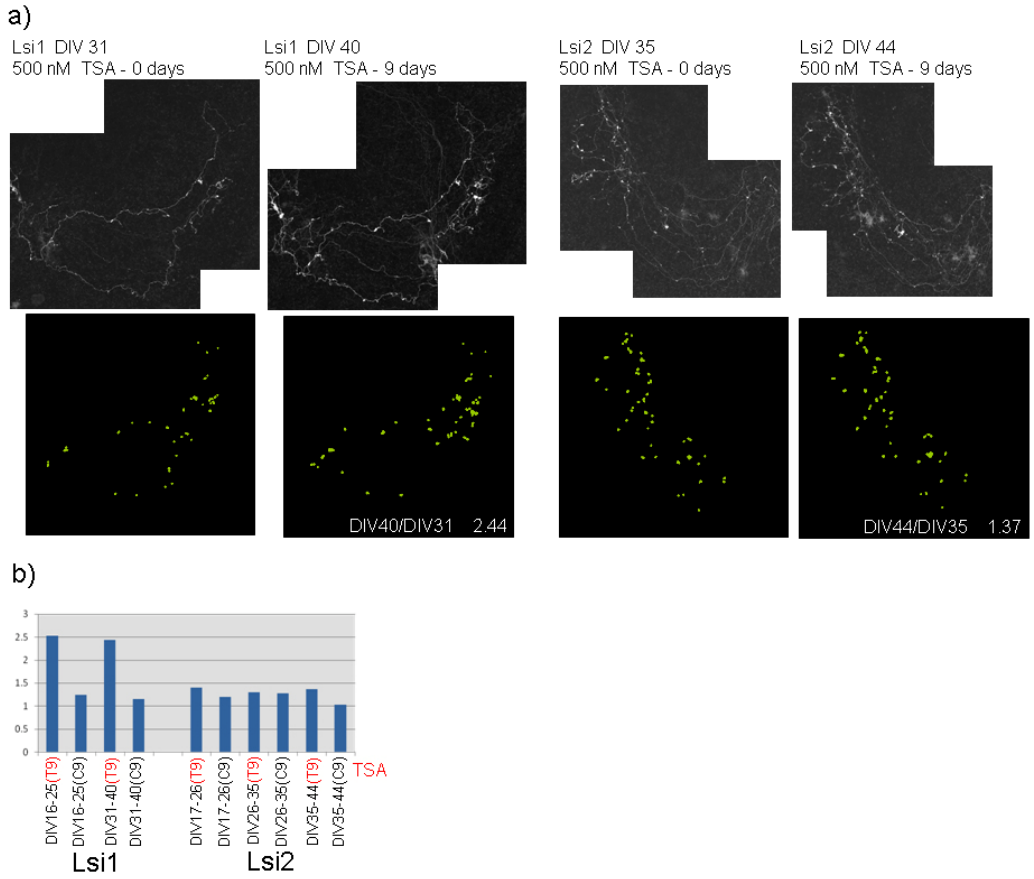

Figure 6. TSA increased volume of mossy fiber terminals in hippocampal slice cultures
a) time-lapse images and drawing of large mossy fiber terminals
b) ratios of total terminal areas between two different time points (later time point/ earlier time point)

Previous studies in the lab have demonstrated that environmental enrichment increases the morphological complexities of large mossy fiber terminals in Lsi1 mice (Galimberti, 2006) (Fig.7).

For example, the number of satellite terminals of large mossy fiber terminals was increased after the environmental enrichment (Galimberti, 2006) (Fig.7).

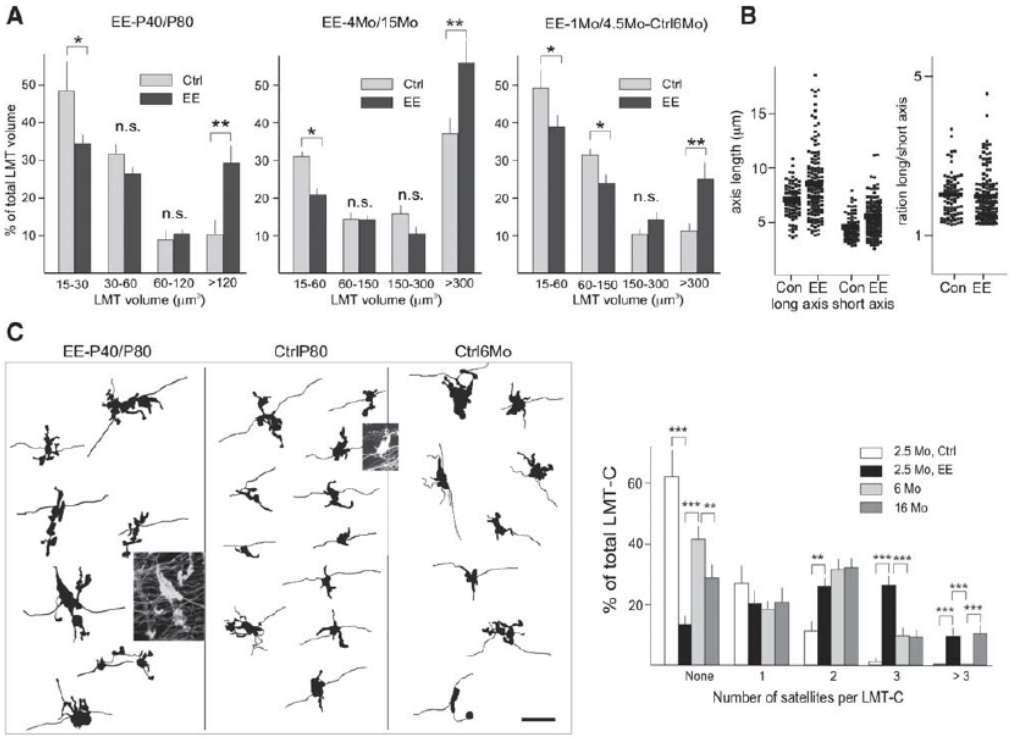

Figure 7. morphological changes of large mossy fiber terminals after environmental enrichment (from Galimberti 2006)

Since environmental enrichment induced the acetylation of histones in the hippocampus, this gave rise to the question whether the HDAC inhibitor treatment in hippocampal slice cultures mimicked the effect of environmental enrichment *in vivo*. To address this question, a detailed morphological analysis was performed for GFP-positive large mossy fiber terminals in Lsi1 slice cultures. Indeed, the numbers of satellite terminals were increased after the TSA treatment (Fig.8).

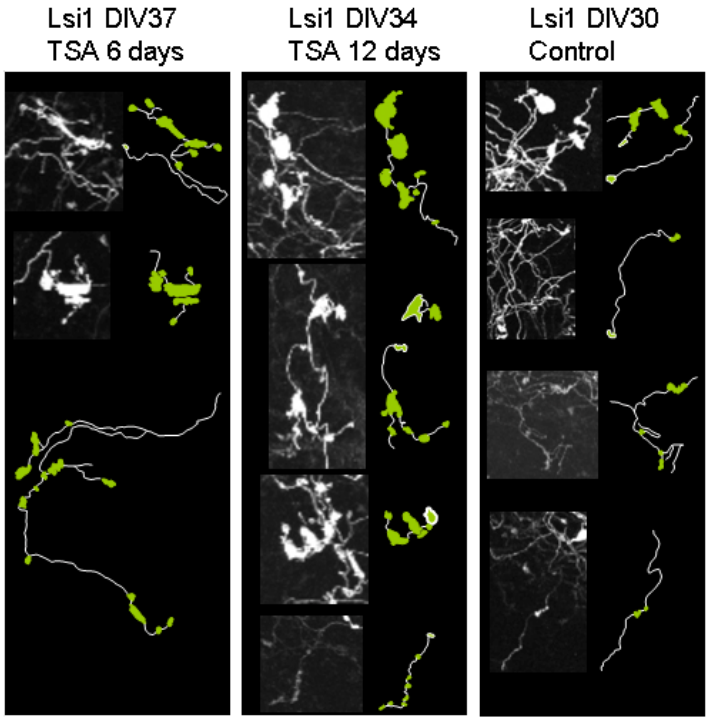

Figure 8. increase of satellite terminals after the TSA treatment
green: satellite terminals, green with the white outline: core terminals which are on the main axon

Microtubule-associated protein 2 (MAP2) is known to be up regulated in the hippocampus after the environmental enrichment (Fischer, 2007). In hippocampal slice cultures, the TSA treatment also enhanced MAP2 protein levels in the dendritic regions of CA3 and CA1 pyramidal cells, but not in the dendritic region of granule cells (Fig.9). Since hippocampal slices were cultured without the entorhinal cortex, the absence of MAP2 up regulation upon TSA in granule cells may be due to an absence of synaptic afferents to these neurons.

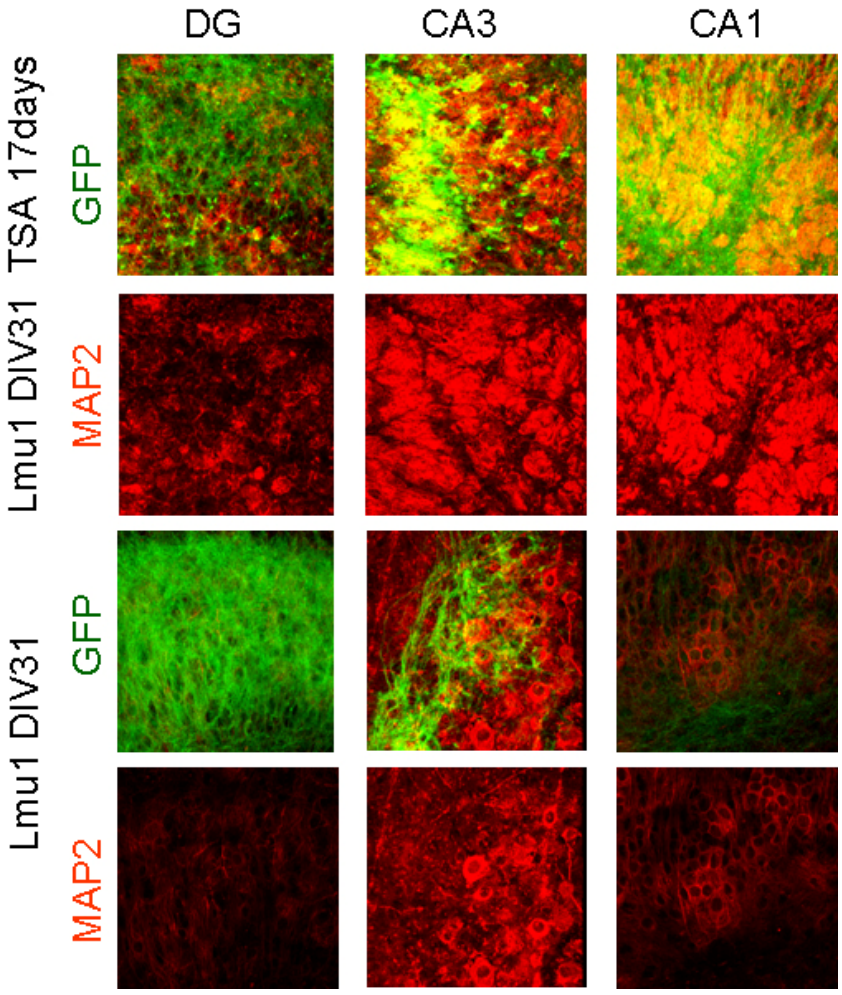

Figure 9. MAP2 staining after TSA treatment in hippocampal slice cultures

2.2.4 Sexual dimorphisms in the hippocampus

Animals have evolved innate beheviours that result in stereotyped social and sexual responses to the environment. Despite dramatic behavioral differences between the sexes, the anatomical and molecular mechanisms underlying these differences are poorly understood.

By doing *in situ* hybridization for GFP, we found that there were consistently many more GFP-positive cells in 8 weeks old Lsi1 female mice than in 8 weeks old Lsi1 male mice (Fig.10).

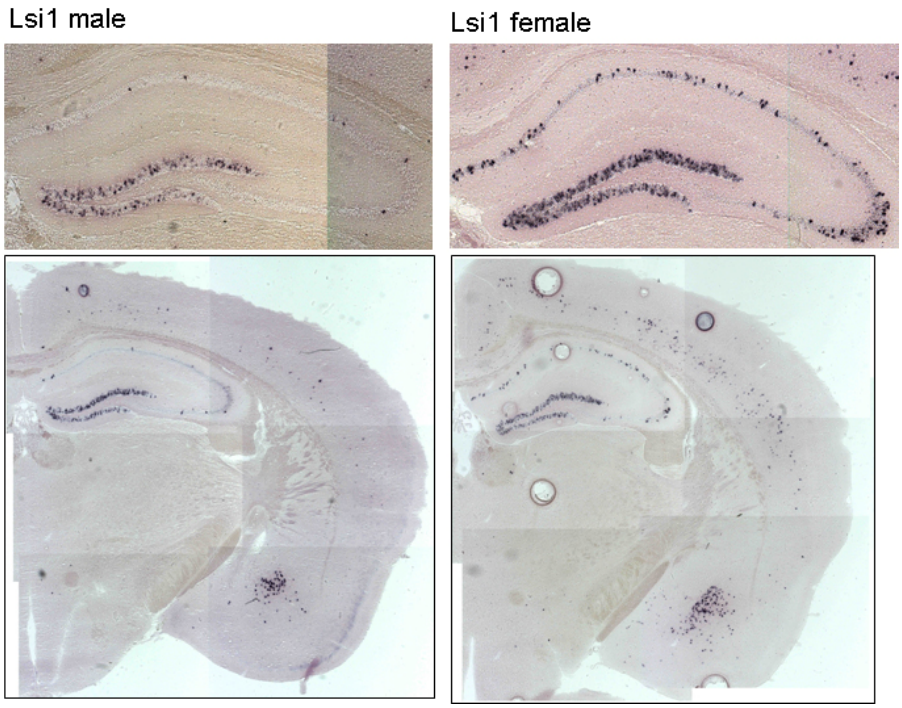

Figure 10. the distribution patterns of GFP-positive cells in adult Lsi1

Furthermore, there were GFP-positive cells in the layer 1-3 of the cortex and the inner CA3 pyramidal cell layer only in 8 weeks old Lmu1 female mice but not in 8 weeks old Lmu1 male mice (Fig.11)

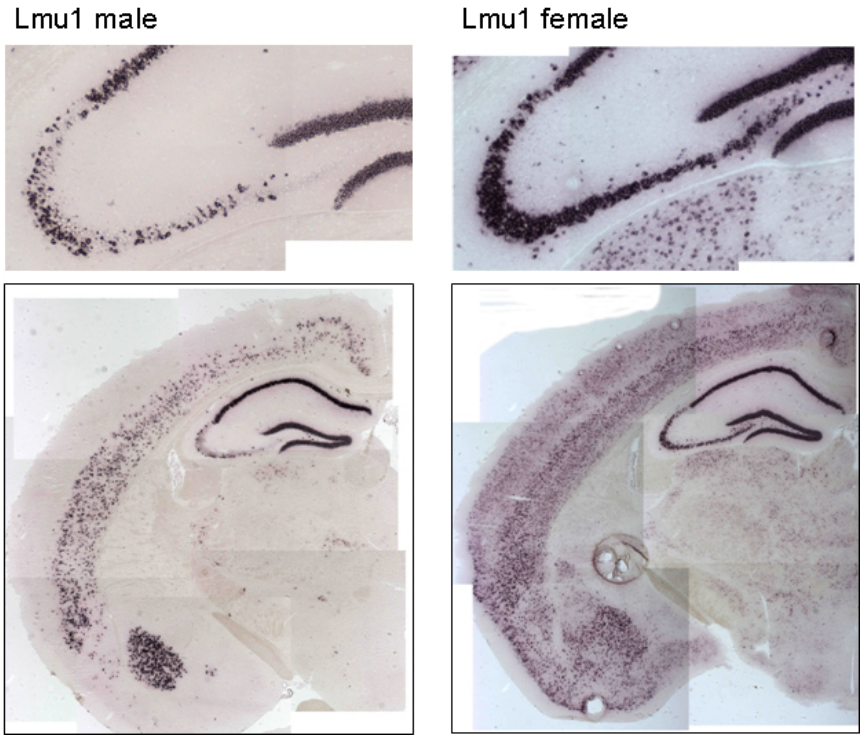

Figure 11. the distribution patterns of GFP-positive cells in adult Lmu1

By contrast, the difference for the number of GFP-positive cells was not pronounced between 2 weeks old Lsi1 male and female mice (Fig.12).

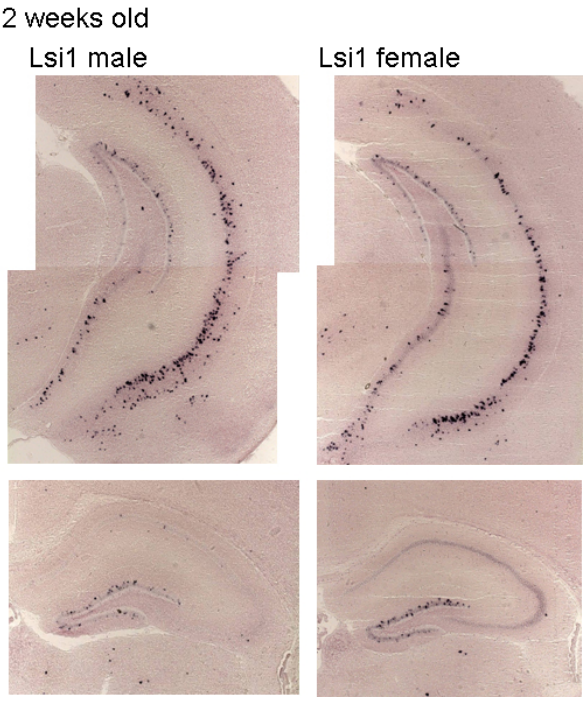

Figure 12. the distribution patterns of GFP-positive cells in 2 weeks old Lsi1 mice

And the distribution patterns of GFP-positive cells were similar in 8 weeks old Lsi2 male and female mice (Fig.13). This suggests that the Thy1 promoter is not just more active in female transgenic mice than in male transgenic mice.

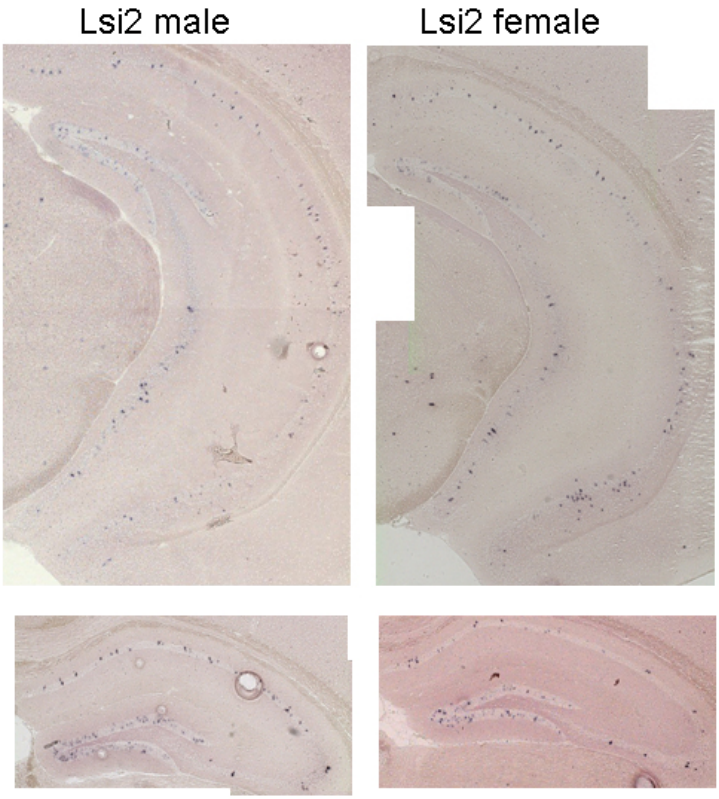

Figure 13. the distribution patterns of GFP-positive cells in adult Lsi2 mice

Microarray analyses were performed for the GFP-positive granule cells, CA3 and CA1 pyramidal cells in Lsi1 female mice to investigate whether GFP-positive cells in the Lsi1 female have similar gene expression patterns to those in Lsi males. The results were that many shared genes which were co-regulated among GFP-positive cells in different regions of Lsi1 male were also co-regulated in the same manner among GFP-positive cells in different regions of Lsi1 female (Fig.14). Furthermore, a hierarchical tree generated for each line and time point based on 679 genes which are the sum of top 100 highest fold change genes from 9 comparisons with random samples (male Lsi1 or Lsi2; DG, CA3 and CA1 and female Lsi1; DG, CA3, CA1; 221 genes were overlapped) showed that GFP-positive cells in Lsi1 female mice were more similar to GFP-positive cells in Lsi1 male mice than those in Lsi2 male mice, or in average principal neurons (Fig.14).

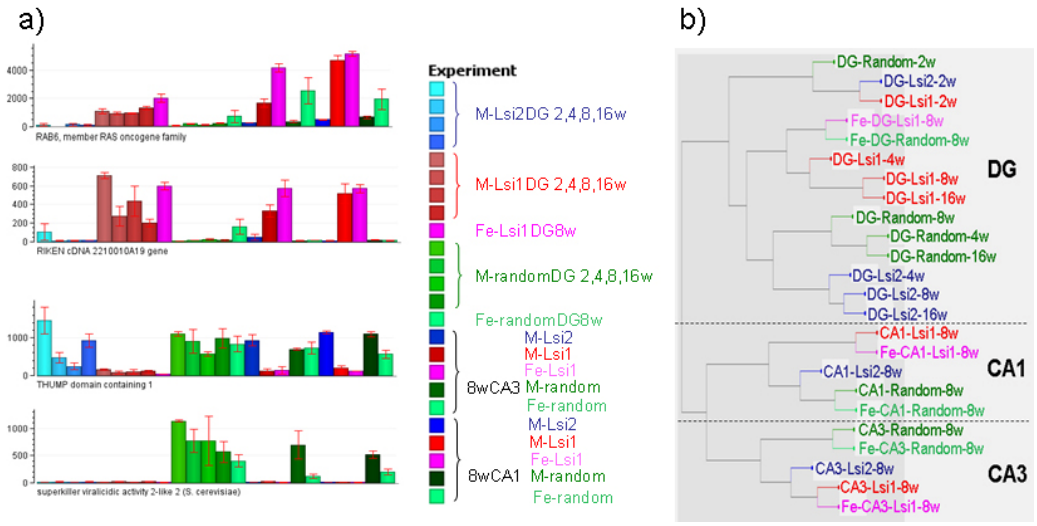

Figure 14. gene expression analysis of GFP-positive cells in Lsi1 female mice
a) expression value of shared genes M; male mice, Fe; female mice
b) hierarchical tree

Interestingly, there were also genes exhibiting distinct expression patterns in males and females. For example, the genes which were down regulated in granule cells from 2 weeks to 16 weeks old male mice exhibited still high expression values like granule cells of 2 weeks old male in granule cells, CA3 and CA1 pyramidal cells of 8 weeks old female mice (Fig.15). In addition, genes which were up regulated in granule cells from 2 weeks to 16 weeks in male mice exhibited low expression values in granule cells, CA3 and CA1 pyramidal cells of 8 weeks old female mice (Fig.15). By contrast, typical developmental genes such as doublecortin were down regulated at 8 weeks in both male and female mice (Fig.15).

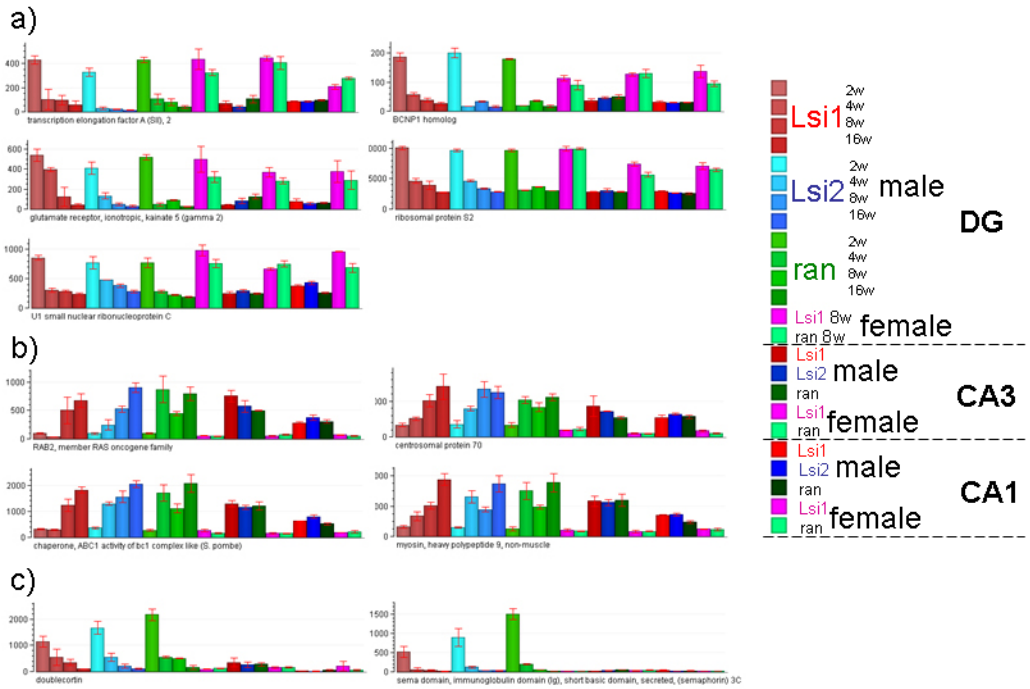

Figure 15. gene expression pattern of hippocampal principal neurons in male and female
a) genes were down regulated from 2 weeks to 16 weeks in granule cells of male mice.
b) genes were up regulated from 2 weeks to 16 weeks in granule cells of female mice.
c) developmentally down regulated genes

About one third of the genes up regulated in female mice (compared with male mice at 8 weeks of age) overlapped with the genes up regulated in 2 weeks old male mice (compared with 16 weeks old male mice) (Fig.16). By contrast, less than 5 % of the genes up regulated in female mice overlapped with the genes down regulated in 2 weeks old male mice (Fig.16). The genes down regulated in female mice also exhibited a similar trend.

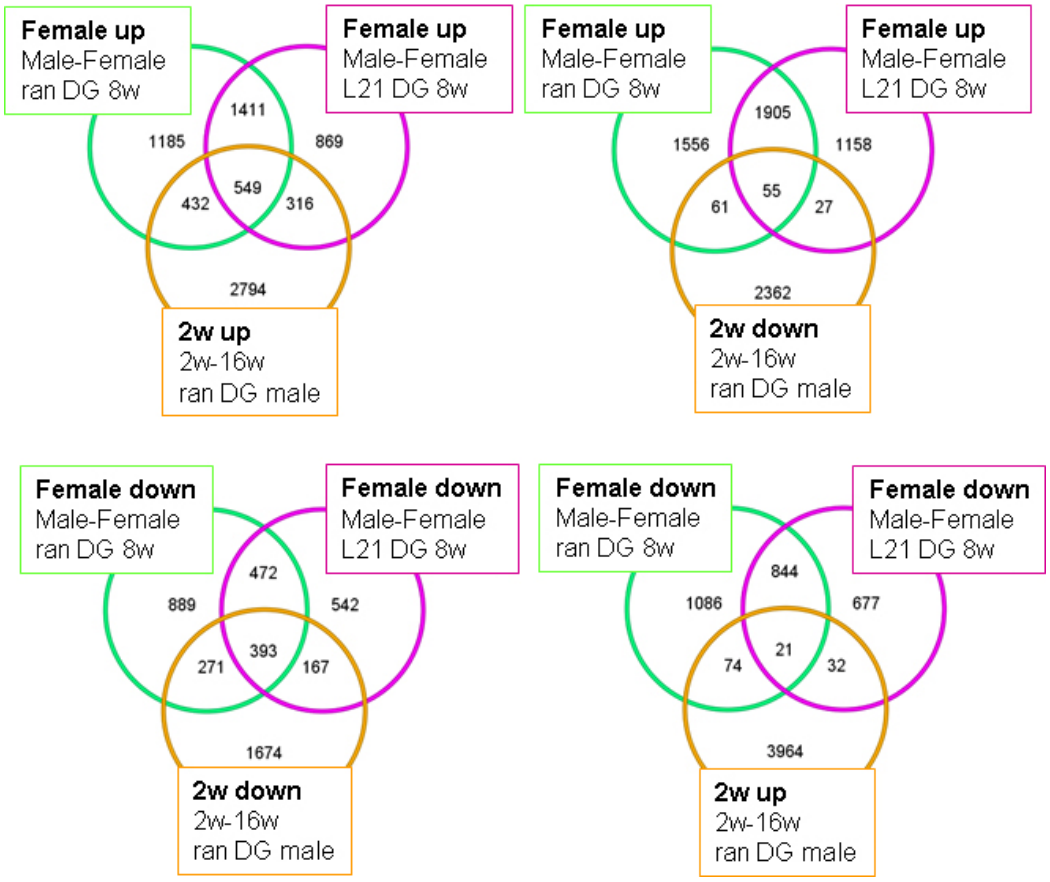

Figure 16. overlap between sexual dimorphism genes and developmentally regulated genes
Genes were calculated based on the T-Test ($p<0.05$, more than 2 fold) between male and female (Male-Female) or between 2 weeks and 16 weeks (2w-16w).

3. Discussion and Conclusion

3.1 The subpopulations in the hippocampus

In this thesis, it was demonstrated that there are subpopulations of principal neurons in the hippocampus. They were identified through gene expression patterns, the timing of neurogenesis, preferential connectivity within the subpopulation, and distinct distribution patterns throughout the whole hippocampus. Since there was no GFP-positive cell in some hippocampal molecular subdomains in Lsi1 or Lsi2 mice, this suggests that molecular domains of the hippocampus may consist of different combinations of neuronal subpopulations. However, it is totally unclear whether these subpopulations may have distinct functional significance. In the nervous system, subpopulations of neurons often exhibit distinct connectivity, which may relate to the specific function of that subpopulation. For example, there were at least two different subpopulations: 'Fear neurons' and 'Extinction neurons' in the basal amygdala classified according to the activity patterns during freezing behaviour (Herry et al., 2008). It was shown that Fear neurons received the input from the ventral hippocampus whereas Extinction neurons did not (Herry et al., 2008). These two subpopulations had distinct connectivity to other brain regions.

It is known that the functions and connectivity to other brain regions are not exactly the same from dorsal to ventral hippocampus (Sahay and Hen, 2007). And GFP-positive CA3 and CA1 pyramidal cells in Lsi1 or Lsi2 were not distributed homogenously throughout the hippocampus. Therefore, there is the possibility that the GFP-positive subpopulation in Lsi1 or Lsi2 might have distinct functions and connectivity. CA1 pyramidal cells in the ventral hippocampus are known to have more connectivities with amygdala than CA1 pyramidal cells in the dorsal hippocampus. In fact, in Lsi1 mice, there were more GFP-positive CA1 pyramidal cells in the ventral hippocampus than in the dorsal hippocampus. By contrast, in Lsi2 mice, there were more GFP-positive CA1 pyramidal cells in the dorsal hippocampus. Therefore, it would be interesting to investigate whether GFP-positive CA1 pyramidal cells in Lsi1 mice may tend to establish connectivity with the amygdala, whereas GFP-positive CA1 pyramidal cells in Lsi2 mice may not. If these two subpopulations should have different connectivities, this would imply that they also have distinct functions.

In a related study, GFP-positive granule cells in Lsi1 mice differed from GFP-positive granule cells in Lsi2 in terms of the number of highly plastic terminals (Galimberti, submitted). Likewise, the morphological responses to an HDAC inhibitor were different between GFP-positive granule cells in Lsi1 and Lsi2 in hippocampal slice cultures. Taken together, these observations suggest that these two subpopulations of principal neurons in the hippocampus may have distinct roles in learning and memory.

3.2 Genetic backbones of subpopulations

Surprisingly, GFP-positive hippocampal principal neurons in Lsi1 or Lsi2 shared co-regulated genes among the different subregions: DG, CA3 and CA1. This suggests that there are particular transcriptional regulation mechanisms which control transgene expression, and that these mechanisms also influence transcriptional regulation of subpopulation specific genes. In other words, each subpopulation could underlie slightly different gene regulatory environments. GFP signals were detectable already in embryonic stages of Lsi1 or Lsi2 mice. Furthermore, the cell type specificities of GFP expression patterns was maintained in Lsi1 or Lmu1-reeler mutant mice, which exhibited the expected disruptions in the cell layering of hippocampus and neocortex (Rakic and Caviness, 1995). It was shown that even neuronal stem cells in the subventricular zone are not homogenous, and prespecify the fate of the neurons they produce (Merkle, et al., 2007). Accordingly, our findings are consistent with the possibility that the fate of the principal neuron subpopulations in the hippocampus is already predetermined genetically before neuronal circuits are set up.

3.3 Genetic approach to dissect the neuronal circuits

I have shown that GFP-positive cells in Lsi1 or Lsi2 mice are not labeled randomly, but instead reflect the existence of specific subpopulations in the hippocampus. However, the mechanism of transgene expression in these mice remains poorly understood. If the expression of transgenes could be controlled in a specific and predictable manner, this would provide valuable tools for the functional analysis of neuronal subpopulations by expressing Cre-recombinase, channelrhodopsins or other functional proteins as a transgene in a specific manner.

Here I showed that the constructs in Lsi1 or Lsi2 mice had inserted in the vicinity of OR gene clusters, whereas the construct in Lmu1 mice did not. OR genes are distributed to around 50 gene clusters at different loci on mouse genome (Godfrey et al., 2004). Each olfactory sensory neuron expresses only one OR gene, and silences all the other OR genes by an unknown mechanism. OR genes are thus highly regulated in a subpopulation specific manner. Surprisingly almost all other known subpopulation markers in the retina, dorsal root ganglia (DRG) neurons and the cerebellum were also located in the vicinity of OR genes on the mouse genome as well as the human genome. This suggests that the unknown mechanism which regulates expression patterns of OR genes could work not only in the olfactory system but also in many brain structures. Therefore, the genomic region in the vicinity of OR gene could exhibit subpopulation specific regulation properties. At this point, it is not possible to say what the mechanism for this regulation may be. Nevertheless, these findings suggest testable ways to generate transgenic mice which express the transgene only in certain subpopulations of neurons in the nervous system. Also in addition, these findings may help to identify subpopulation specific marker genes by determining whether candidate genes are in the vicinity of an OR gene cluster.

3.4 Sexual dimorphisms in the hippocampus

There are published reports of sexual dimorphisms in the hippocampus. For instance, the number of granule cells of the hippocampus in females is smaller than in males, and this number depended on gonadal hormone levels (Tabibnia et al., 1999; Galea et al., 1999). Furthermore, the numerical density of synapses between mossy fiber terminals and apical dendritic excrescences of CA3 was higher in the female rat hippocampus than in male (Maderia et al., 1991). Moreover, sex differences have been reported in hippocampal-dependent learning and memory. For example, male mice exhibited better spatial working and reference memory than female mice (Gresack and Frick 2003). There were also different behavioral responses between male and female rats in contextual fear memory tests (Gresack et al., 2009). Finally, morphological changes in response to chronic glucocorticoid stress were different between male and female mice (Liu et al., 2006): after 2 weeks of elevated corticosterone levels, the total length and branch points of apical dendrites of CA3 pyramidal cells in male mice were decreased, but those in females were increased (Liu et al., 2006). Thus, the hippocampus can respond in different ways in male and female mice. However, the basis for these differences between male and female hippocampus is not understood.

One possibility is that the properties of many principal neurons in the hippocampus are slightly different between male and female mice and/or that the compositions of subpopulations are different. Here I show that there are more GFP-positive cells in adult Lsi1 female than adult Lsi1 males, and that these GFP-positive cells in Lsi1 females expressed Lsi1 specific marker genes in a similar way to those in Lsi1 males. Furthermore, some of the genes which were up regulated in Lsi1 GFP-positive cells were detected at higher levels in pools of average neurons in female mice than in male mice. This suggests that the proportion of the Lsi1 subpopulation may be higher in the hippocampus of female mice compared with male mice.

What could be the mechanism underlying this observation? Around 6000 genes were up or down regulated more than 2 fold between granule cells of 2 weeks old male and 16 weeks old male mice. Interestingly, around 20 % the genes up-regulated in 2 weeks compared with 16 weeks overlapped with genes up-regulated in 8 weeks old females compared with 8 weeks old males. In addition, there was much less overlap between genes up-regulated in 2 weeks (compared with 16 weeks) and genes up-regulated in 8 weeks old males (compared with female). In other words, some of the

transcriptional changes that took place between 2 weeks old males and adult males did not take place in female mice, where these genes maintained their 2 weeks expression levels in adult female mice. Furthermore, the difference in the number of GFP-positive cells between 2 weeks old Lsi1 male and female mice was not pronounced. Since gonadal hormones like testosterone usually start to be secreted from puberty on, these time courses suggested a role for gonadal hormones in bringing about these differential regulations. Accordingly, the additional fraction of GFP-positive cells in Lsi1 female mice might reflect gonadal hormone regulation. One report has demonstrated that neonatal testosterone treatment of rat females resulted in a more male-like hippocampus in terms of the shape of granule cell layers, and the performance in a spatial navigation task (Roof, 1992). Therefore, it would be interesting to determine whether the injection of testosterone can alter the expression patterns of GFP-positive cells especially in Lsi1 or Lmu1 females, and also the composition of subpopulations in the hippocampus. In a more ambitious context, this might also change the connectivity properties between the hippocampus and the amygdala.

3.5 Conclusions and further consideration

What is the most exciting moment in science? There could be many answers. I would like to say that one of them is to find the 'unexpected' interesting thing. I think that a human brain may not be smart enough to predict what evolution has been generating for billions of years. That is why 'unexpected' findings could be so important.

In this thesis, the first unexpected finding was the specific GFP expression patterns in Lsi1, Lsi2 or Lmu1 mice. The endogenous thymus cell antigen 1, theta (Thy1) gene is highly expressed in almost all neurons including all granule cells, CA3 and CA1 pyramidal cells in the hippocampus. One could think that almost all neurons express the transgene when the Thy1 promoter is used for transgene expression. In fact, only a few principal neurons in the hippocampus were GFP-positive in Lsi1 or Lsi2 mice. And more interestingly, these GFP-positive cells were not labeled randomly but reflecting specific subpopulations revealed by gene expression analysis, distinct distributions of GFP-positive cells and timing of neurogenesis.

The second unexpected finding was that the GFP-positive cells in Lsi1 or Lsi2 mice shared common properties such as gene expression patterns and the timing of neurogenesis among different subregions in the hippocampus. The GFP-positive granule cells tend to exhibit preferential connectivity to GFP-positive CA3 pyramidal cells in Lsi1 or Lsi2 probably due to these common properties. Intriguingly, some of these co-regulated subpopulation specific genes were alternative splicing variants. Since 3' UTR arrays were used for this microarray analysis, splicing variants were only detectable if they exhibited differences in their 3' UTR. Therefore, it is possible that more alternative splicing variants are shared among GFP-positive cells of different subregions in Lsi1 or Lsi2. If splicing variants of cell adhesion molecules are also shared, this might also contribute to establish preferential connectivity between GFP-positive cells.

The third unexpected finding was that there was subpopulation specific regulation in the vicinity of OR gene clusters. OR genes are known to be regulated in a subpopulation specific manner. However, so far, there had been no evidence suggesting that loci in the vicinity of OR gene clusters may be regulated in a subpopulation specific manner. I have shown here that known subpopulation specific marker genes mapped in the vicinity of OR gene clusters whereas broad cell type marker genes did not. However, subpopulation marker genes specific for

developmental stages were not correlated OR gene clusters. This suggests that chromatin structures or other epigenetic modifications in immature neurons may not yet be set up like in mature neurons, and that many subpopulation specific gene regulation properties become effective in mature neurons to contribute to the properties of neuronal subpopulations in the adult.

4. Supplementary Materials and methods

4.1 Microarray analysis

Microarray analysis was done using the data analysis software Expressionist (Genedata, Basel, Switzerland). The hierarchical tree was calculated based on the median values of the each experiment by the clustering tool of Expressionist.
The distance analysis for olfactory receptor genes was performed using *Mus musculus* (build 37.1) and *Homo sapiens* (build 36.3) genome data (National Center for Biotechnology Information, NCBI).

4.2 In situ hybridization

In situ hybridization was done by the standard nonradioactive protocol. Brains were frozen in 2-methylbutane. The thickness of frozen sections was 20 μm. Probes were labeled by digoxigenin (DIG). The color reaction was detected by the NBT/BCIP reaction.

Sequences of probes for the *in situ* hybridization

GFP

GCGGGGATCCGTGAGCAAGGGCGAGGAGCTGTTCACCGGGGTGGTGCCC
ATCCTGGTCGAGCTGGACGGCGACGTAAACGGCCACAAGTTCAGCGTGTC
CGGCGAGGGCGAGGGCGATGCCACCTACGGCAAGCTGACCCTGAAGTTCA
TCTGCACCACCGGCAAGCTGCCCGTGCCCTGGCCCACCCTCGTGACCACCC
TGACCTACGGCGTGCAGTGCTTCAGCCGCTACCCCGACCACATGAAGCAG
CACGACTTCTTCAAGTCCGCCATGCCCGAAGGCTACGTCCAGGAGCGCAC
CATCTTCTTCAAGGACGACGGCAACTACAAGACCCGCGCCGAGGTGAAGT
TCGAGGGCGACACCCTGGTGAACCGCATCGAGCTGAAGGGCATCGACTTC
AAGGAGGACGGCAACATCCTGGGGCACAAGCTGGAGTACAACTACAACA
GCCACAACGTCTATATCATGGCCGACAAGCAGAAGAACGGCATCAAGGTG
AACTTCAAGATCCGCCACAACATCGAGGACGGCAGCGTGCAGCTCGCCGA
CCACTACCAGCAGAACACCCCCATCGGCGACGGCCCCGTGCTGCTGCCCG
ACAACCACTACCTGAGCACCCAGTCCGCCCTGAGCAAAGACCCCAACGAG
AAGCGCGATCACATGGTCCTGCTGGAGTTCGTGACCGCCGCCGGGATCAC
TCTCGGCATGGACGAGCTGTACAAGTAAAGCGGCCGCCTCGAGGGCGC

Stx3-sv1 (NM_011502 or NM_001025307)

ACACAGCCTGAAGGCCAGGATGGTGGTGAAGAGGCAGGCATTACAACAT
GCCCAACTCAACAGGGTCATACTGAACTCAGTGAGGCTGTCTCTCAGATC
ATGGTACTCCCTACTTTTACTCTAATGGCTCTTCTAGGTCGCATTCTTAACC
AACCACATGTCTGCTTCCTCTTTCAGGGTCCAAGAATAGTTTTTAATTCAT
AGATTGTTTAAGGATAGGCACTATGCCTATCTCGAATACTACCATGTCCCT
TCTCTTAGCACACAGTGCCTGCCACTTTCAGATGTCTGCTTACTTATAGTC

AAGCTTTGATTTCATTCATGGATGAGTCTTTGAGCTTGGCTTTTAACTCTTT
AAGGTACCATTGGGAACATGATTTTTTATTAATCAGAGGCACATAGAAAA
ATATGGCAACACCCCTATTACCATACCATACCTGTCACAGTGTTCTGTTTT
GAGGGATGGTGCTTATGTAGAAGCTGGCTTTGTATTGATGGTATAAATTTC
TATTAGTACTCTCATTTGTCAGAGATGATAGTTGGTCTCAGGATGGAGGTT
CATTCAATAAATTCATTCCTCCAACAAAAGAAAGAAGTTTATACTATGAC
CCAGCTCCCAAACAAGCACACCATGTTATCTGGAACAATGGAAGGAAGCC
AAGGGGATAAAGTGGGACGAGGCTGCTGCTTCAGCCTCACCATGTCTGTG
GTAGAATAGGCTGCAGGTCAGTGAAATGTGCAAGAAACTGGTCCAAACAC
ATTTCTAACTCAAGTGTCACTGTGTTCCACTTTAAAAATAATTTACTTTGA
GACTATTACATTTTACATTCATTAAAAATAAATGAAAATCTGCGTCTAACT
TTTGAAAGTAAGTGTTAACTTACTTGAATGCTGGTTCCCCCAGAAAAACTG
ATTACTCTTGTTACGGACAAATGAAGCTGGCACCATGA

Rps9

CCCGGGAGCTGTTGACGCTAGACGAGAANGAATCCCGGCGTNNNNTTNNA
GNCAANNCTNNCCTGNGGCGGCTTNTTCNCATTGGGGTGCTGGACGAGGG
CAAGATGAAGCTGGATTACATCCTGGGCCTGAAGATTGAGGATTTCTTGG
AGAGGCGGCTGCAGACCCAGGTCTTTAAGCTGGGCCTGGCCAAATCTATT
CACCATGCCCGTGTGCTCATCCGCCAACGTCACATTAGGGTCCGCAAGCA
GGTGGTGAACATCCCATCCTTCATTGTTCGCCTGGACTCTCAGAAGCACAT
CGACTTCTCCCTCCGTTCTCCTTATGGCGGCGNCCGTCCAGGCCGAGTGAA
GAGGAAGAATGCCAAGAAAGGCCAGGGCGGGGCTGGAGCTGGTGATGAT
GAGGAAGAGGATTAATTAATACTTGGCTGAACTGGAGGATTGTCT

4.3 3D reconstruction of the adult hippocampus

In situ hybridization for GFP was performed according to a standard protocol, using digoxigenin-labeled probes for nonradioactive detection. Consecutive coronal sections were cut at 20 μm throughout a whole hippocampus. Pictures were aligned using AutoAligner (Bitplane AG). Spots were put and the contour surface of the CA3 pyramidal cell layer was drawn manually using the 3D/4D image analysis software Imaris (Bitplane AG).

4.4 FISH (Fluorescence in situ hybridization)

The FISH experiments were performed by SeeDNA (Ontario, Canada).
Chromosomal spreads preparation: Lymphocytes were isolated from the spleen of a mouse and cultured at 37 ˚C in RPMI 1640 medium supplemented with fetal calf serum, concanavalin A, lipopolysaccharide and mercaptoethanol. The mouse cells

were harvested and chromosomal slides were made by conventional method preparation including hypotonic treatment, fixation and air dry.

Probe labeling, *in situ* hybridization and dual color FISH detection: DNA probe for GFP was labeled by Digoxigenin (Heng et al, 1992). The procedure for hybridization and detection was performed according to Heng et al., 1992; Heng et Tsui, 1993. Briefly, slides were baked at 55˚C for 1 hour. After RNase treatment, the slides were denatured in 70 % formamide in 2xSSC followed by dehydrated with ethanol. Probes were denatured in a hybridization mix consisting of 50% formamide and 10% dextran sulphate. The probe was loaded on the denatured chromosomal slides. After over night hybridization, the slide was washed and detected as well as amplified (Heng, 1993). Digoxigenin labeled probe was detected by Rhodamine.

Image analysis: FISH signals were observed under fluorescent microscopy. Images were captured by CCD camera and merged by RS Image software.

4.5 Hippocampal slice culture

Hippocampal slice cultures, long-term live imaging of slice cultures and staining for hippocampal slices were performed according to these protocols (Gogolla et al., 2006; Gogolla et al., 2006; Gogolla et al., 2006). The final concentration of TSA was 500 nM in the culture medium. When culture medium was changed every 3 days, new TSA was added into the culture medium and stayed for next 3 days.

5. References

Andersen P., Morris R., Amaral, D., Bliss, T. and O'Keefe, J. (2007) The Hippocampus Book. Oxford university press 46

Buck, L., and Axel, R. (1991) A novel multigene family may encode odorant receptors: a molecular basis for odor recognition. *Cell 65*, 175-187

Caroni, P. (1997) Overexpression of growth-associated proteins in the neurons of adults transgenic mice. *J. Neuroscience Method* 71, 3-9

Feng, G., Mellor, R. H., Bernstein, M., Keller-Peck, C., Nguyen, Q. T., Wallace, M., Nerbonne, J. M., Lichtman, J. W. and Sanes, J. R. (2000) Imaging neuronal subsets in transgenic mice expressing multiple spectral variants of GFP. *Neuron* 28, 41-51

Fischer, A., Sananbenesi F., Wang, X. Dobbin, M. and Tsai, L. H. (2007) Recovery of learning and memory is associated with chromatin remodelling. *Nature* 447, 178-183

Galea, L. A. M., Perrot-Sinal, T. S., Kavaliers, M. and Ossenkopp K. P. (1999) Relations of hippocampal volume and dentate gyrus width to gonadal hormone levels in male and female meadow voles. *Brain Res.* 821, 383-391

Galimberti, I., Gogolla, N., Alberi, S., Santos, A. F., Muller, D. and Caroni, P. (2006) Long-term rearrangements of hippocampal mossy fiber terminal connectivity in the adult regulated by experience. *Neuron* 50, 749-763

Godfrey P. A., Malnic, B. and Buck, L.B. (2004) The mouse olfactory receptor gene family. *Proc. Natl Acad. Sci. USA* 101, 2156-2161

Gogolla, N., Galimberti, I., De Paola, V., Caroni, P. (2006). Preparation of organotypic hippocampal slice cultures for long-term live imaging. *Nature Protocols* 1, 1165-1171

Gogolla, N., Galimberti, I., De Paola, V., Caroni, P. (2006). Long-term live imaging of neuronal circuits in organotypic slice cultures. *Nature Protocols* 1, 1223 – 1226

Gogolla, N., Galimberti, I., De Paola, V., Caroni, P. (2006). Staining protocol for organotypic hippocampal slice cultures. *Nature Protocols* 1, 2452 – 2456

Gresack, J. E. and Frick, K. M. (2003) Male mice exhibit better spatial working and reference memory than females in a water-escape radial arm maze task. *Brain Res.* 982, 98-107

Gresack, J. E., Schafe, G. E., Orr, P. T. and Frick, K. M. (2009) Sex differences in contextual fear conditioning are associated with differential ventral hippocampal extracellular signal-regulated kinase activation. *Neuroscience* 159, 451-467

Guan L. S., *et al* (2009) HDAC2 negatively regulates memory formation and synaptic plasticity. *Nature* 459, 55-63

Hampson, R. E., Heyser C. J. and Deadwyler, S. A. (1993) Hippocampal cell firing correlates of delayed-match-to-sample performance in the rat. *Behav. Neurosci.* 107, 715-739

Heng HHQ, Squire J, Tsui L-C (1992) High resolution mapping of mammalian genes by in situ hybridization to free chromatin. *Proc Natl Acad Sci USA* 89, 9509-9513

Heng HHQ and Tsui L-C (1993) Modes of DAPI banding and simultaneous in situ hybridization. *Chromosoma* 102, 325-332

Herry, C., Ciocchi, S., Senn, V., Demmou, L., Müller, C and Lüthi, A. (2008) Switching on and off fear by distinct neuronal circuits. *Nature* 454, 600-606

Jessell, T. M. (2000) Neuronal specification in the spinal cord: inductive signals and transcriptional codes. *Nature rev. Genetics* 1, 20-29

Kamme, F., Salunga, R., Yu, J., Tran, D. T., Zhu, J., Luo, L., Bittner, A., Guo, H. Q., Miller, N., Wan, J. and Erlander, M. (2003) Single-cell microarray analysis in hippocampus CA1: demonstration and validation of cellular heterogeneity. *J. neuroscience* 23, 3607-3615

Kjelstrup, K. B., Solstad, T., Brun, V. H., Hafting, T., Leutgeb, S., Witter, M. P., Moser, E. I. amd Moser, M. B. (2008) Finite scale of spatial representation in the hippocampus. *Science* 321, 140-143

Lee, A.K. and Wilson, M. A. (2002) Memory of sequential experience in the hippocampus during slow wave sleep. *Neuron* 36, 1183-1194

Lein, E. L., Zhao, X. and Gage, F. H. (2004) Defining a molecular atlas of the hippocampus using DNA microarrays and high-throughput *in situ* hybridization. *J. neuroscience* 24, 3879-3889

Lein, E. L. *et al.* (2007) Genome-wide atlas of gene expression in the adult mouse brain. *Nature* 445, 168-176

Livet, J., Weissman, T. A., Kang, H., Draft, R. W., Lu, J., Bennis, R. A., Sanes, J. S. and Lichtman J. W. (2007) Transgenic strategies for combinatorial expression of fluorescent proteins in the nervous system. *Nature* 450, 56-63

Liu, H. H., Payne, H. R., Wang, B. and Brady, S. T. (2006) Gender differences in response of hippocampus to chronic glucocorticoid stress: role of glutamate receptors. *J. Neurosci. Res.* 83, 775-786

Maderia, M. D., Sousa, N. and Paulabarbosa M. M. (1991) Sexual dimorphism in the mossy fiber synapses of the rat hippocampus. *Exp. Brain Res.* 87, 537-545

Martin, L. A., Tan, S. S. and Goldowitz D. (2002) Clonal architecture of the mouse hippocampus. *J. neuroscience* 22, 3520-3530

Marshall, L., Helgadottir, H., Molle, M. and Born, J. (2006) Boosting slow oscillations during sleep potentiates memory. *Nature* 444, 610-613

McHugh, T. J., Jones, M. W., Quinn, J. J., Balthsar, N., Coppari, R., Elmquist, J. K., Lowell, B. B., Fanselow, M. S., Wilson, M.A. and Tonegawa, S. (2007) Dentate gyrus NMDA receptors mediate rapid pattern separation in the hippocampus network. *Science* 317, 94-99

Merkle, F. T., Mirzadeh, Z. and Alvarez-Buylla A. (2007) Mosaic organization of neural stem cells in the adults brain. *Science* 317, 381-384

Moser, E. I., Kropff E. and Moser, M. B. (2008) Place cells, grid cells, and the brain's spatial representation system. *Annu. Rev. Neurosci.* 31, 69-89

Moser M. B. and Moser E. I. (1998) Functional differentiation in the hippocampus. *Hippocampus* 8, 608-619

Nakazawa, K., Quirk, M. C., Chitwood, R. A., Watanabe, M., Yeckel, M. F., Sun, L. D., Kato, A., Carr, C. A., Johnston, D., Wilson, M. A. and Tonegawa S. (2002) Requirement for hippocampal CA3 NMDA receptors in associative memory recall. *Science* 297, 211-218

Ngai, J., Chess, A., Dowling, M.M., Necles, N., Macagno, E.R., and Axel, R. (1993) Coding of olfactory information: topography of odorant receptor expression in the catfish olfactory epithelium. *Cell 72*, 667-680

O'Keefe, J. and Dostrovsky J. (1971) The hippocampus as a spatial map. Preliminary evidence from unit activity in the freely-moving rat. *Brain Res.* 34, 171-175

Rakic, P. and Caviness, V. S. Jr., (1995) Cortical development: view from neurological mutants two decades later. *Neuron* 14, 1101-1104

Resseler, K.J., Sullivan, S.L., and Buck, L.B. (1994) Information coding in the olfactory system: evidence for a stereotype and highly organized epitope map in the olfactory bulb. *Cell 79*, 1245-1255

Roof, R. L. and Havens, M. D. (1992) Testosterone improves maze performance and induces development of a male hippocampus in females. *Brain Res.* 572, 310-313

Sahay, A. and Hen, R. (2007) Adults hippocampal neurogenesis in depression. *Nature Neuroscience* 10, 1110-1115

Sanguinetto, S. D. T., Dasen, J. S. and Arber, S. (2008) Transcriptional mechanisms controlling motor neuron diversity and connectivity. *Current Opinion in Neurobiology* 18, 36-43

Scoville, W. B. and Milner, B. (1957) Loss of recent memory after bilateral hippocampal lesions. *J. Neurol. Neurosurgery and Psychiatry* 20, 11-21

Tabibnia G., Cooke, B. M. and Breedlove, S. M. (1999) Sex difference and laterality in the volume of mouse dentate gyrus granule cell layer. *Brain Res.* 827, 41-45

Thompson, C L. *et al.* (2008) Genomic anatomy of the hippocampus. *Neuron* 60, 1010-1021

Tsien, J. Z., Huerta, P. T and Tonegawa, S. (1996) The essential role of hippocampal CA1 NMDA receptor-dependent synaptic plasticity in spatial memory. *Cell* 87, 1327-1338

Wässle, H. (2004) Parallel processing in the mammalian retina. *Nature rev. Neuroscience* 5, 1-11

West, M. J., Slomianka, L. and Gundersen H. J. G. (1991) Unbiased stereological estimation of the total number of neurons in the subdivisions of rat hippocampus using the optical fractionator. *Anat. Rec.* 231, 482-497

Zong, H., Espinosa, J. S., Su, H. H., Muzumdar, M. D. and Luo, L. (2005) Mosaic analysis with double markers in mice. *Cell* 121, 479-492

Acknowledgements

First of all, I would like to thank Dr. Pico Caroni for giving a wonderful opportunity for me to challenge interesting projects and to learn how to do the ‘Science’. It’s really an exciting moment to enjoy Science.

I would like to thank Dr. Silvia Arber and Dr. Botond Roska for their efforts as a member of my thesis committee. Their suggestion from a different angle made this project more interestingly.

I would like to thank Dr. Ivan Galimberti and Flavio Donato for the collaboration of this project. Without their efforts, it’s not possible to achieve this project.

I would like to thank also Dr. Erik Cabuy and Dr. Edward Oakeley for microarray experiments and helping to analyze data. Their strong supports helped me a lot.

I would like to thank all the past and present members of Caroni group not only for scientific activities but also for many other things. I’m happy that I could share great time with them.

In the end, I would thank Misuzu for all.

C urriculum Vitae

Yuichi Deguchi

Born the 19th April, 1979
Place of birth: Osaka, Japan
Nationality: Japan

Work address:

Friedrich Miescher Institute for Biomedical Research
Maulbeerstrasse 66
4058 Basel Switzerland
tel: +41 616 97 66 99
fax: +41 616 97 39 76
E-mail address: yuichi.deguchi@fmi.ch

Education and research experience

05/2005-present	Friedrich Miescher Institute (Basel, Switzerland) Ph.D. thesis with Prof. Dr. Pico Caroni 'Genetic diversity of principal neurons in the hippocampus'
04/2003-03/2005	Graduate School of Biostudies, Kyoto university (Kyoto, Japan) Master's thesis with Prof. Dr. Shingo Hata 'Transcriptome profiling of Lotus japonicus roots during arbuscular mycorrhiza development and comparison with that of nodulation'
04/1999-03/2003	Department of applied life science, Faculty of Agriculture, Kyoto University (Kyoto, Japan)

Publications

Gogolla, N., Galimberti, I., Deguchi, Y. and Caroni, P. (2009)
Wnt signaling mediates experience- related regulation of synapse numbers and mossy fiber connectivities in the adult hippocampus.
Neuron 62, 510-525

Deguchi, Y., *et al.* (2007)
Transcritome profiling of Lutus japonicus roots during arbuscular mycorrhiza development and comparison with that of nodulation.
DNA Res. 14, 117-133

Scientific communications
abstract
Deguchi, Y. and Caroni, P. (2008)
Principal neurons in the hippocampus: genetic diversity and patterned distribution.
FENS Forum, Geneva, Switzerland, A9-008.8